OXFORD UNIVERSITY PRESS Journal of Molecular Cell Biology

FSHD muscular dystrophy Region Gene 1 binds Suv4-20h1 histone methyltransferase and impairs myogenesis.

Journal:	*Journal of Molecular Cell Biology*
Manuscript ID:	JMCB-2012-0259.R1
Manuscript Type:	Original Article
Date Submitted by the Author:	n/a
Complete List of Authors:	Neguembor, Maria; San Raffaele Scientific Institute, Division of Regenerative Medicine; Università Vita-Salute San Raffaele, Xynos, Alexandros; San Raffaele Scientific Institute, Division of Regenerative Medicine Onorati, Maria; Universita' degli Studi di Palermo, Dipartimento STEMBIO - Sezione Biologia Cellulare; Dulbecco Telethon Institute, Caccia, Roberta; San Raffaele Scientific Institute, Division of Regenerative Medicine Bortolanza, Sergia; San Raffaele Scientific Institute, Division of Regenerative Medicine Godio, Cristina; San Raffaele Scientific Institute, Division of Regenerative Medicine Pistoni, Mariaelena; San Raffaele Scientific Institute, Division of Regenerative Medicine Corona, Davide; Universita' degli Studi di Palermo, Dipartimento STEMBIO - Sezione Biologia Cellulare; Dulbecco Telethon Institute, Schotta, Gunnar; Ludwig Maximilians University, Munich Center for Integrated Protein Science and Adolf Butenandt Institute Gabellini, Davide; San Raffaele Scientific Institute, Division of Regenerative Medicine; Dulbecco Telethon Institute,
Keyword:	Epigenetics, Muscle, Transcription

FSHD muscular dystrophy Region Gene 1 binds Suv4-20h1 histone methyltransferase and impairs myogenesis

Running head: Epigenetic deregulation by FRG1

Maria Victoria Neguembor[1,2], Alexandros Xynos[1], Maria Cristina Onorati[3], Roberta Caccia[1], Sergia Bortolanza[1], Cristina Godio[1], Mariaelena Pistoni[1], Davide F. Corona[3], Gunnar Schotta[4] and Davide Gabellini[1]

[1] Dulbecco Telethon Institute and Division of Regenerative Medicine, San Raffaele Scientific Institute, 20132 Milano, Italy

[2] Università Vita-Salute San Raffaele, 20132 Milano, Italy

[3] Dulbecco Telethon Institute, Università degli Studi di Palermo, Dipartimento STEMBIO - Sezione Biologia Cellulare, 90128 Palermo, Italy

[4] Munich Center for Integrated Protein Science and Adolf Butenandt Institute, Ludwig Maximilians University, 80336 Munich, Germany

Corresponding author:

Davide Gabellini, Division of Regenerative Medicine, San Raffaele Scientific Institute, DIBIT 2, 5A3-44, Via Olgettina 58, 20132 Milano, Italy. E-mail: gabellini.davide@hsr.it, Telephone +39.02.2643.5934, Fax +39.02.2643.5544

ABSTRACT

Facioscapulohumeral Muscular Dystrophy (FSHD) is an autosomal dominant myopathy with a strong epigenetic component. It is associated with deletion of a macrosatellite repeat leading to over-expression of the nearby genes. Among them, we focused on *FSHD Region Gene 1* (*FRG1*) since its over-expression in mice, *X. laevis* and *C. elegans* leads to muscular dystrophy-like defects, suggesting that *FRG1* plays a relevant role in muscle biology. Here we show that, when over-expressed, FRG1 binds and interferes with the activity of the histone methyltransferase Suv4-20h1 both in mammals and *Drosophila*. Accordingly, *FRG1* over-expression or *Suv4-20h1* knockdown inhibits myogenesis. Moreover, *Suv4-20h* KO mice develop muscular dystrophy signs. Finally, we identify the FRG1/Suv4-20h1 target *Eid3* as a novel myogenic inhibitor that contributes to the muscle differentiation defects. Our study suggests a novel role of FRG1 as epigenetic regulator of muscle differentiation and indicates that Suv4-20h1 has a gene-specific function in myogenesis.

INTRODUCTION

Facioscapulohumeral muscular dystrophy (FSHD, OMIM 158900) is the third most common myopathy, exhibits autosomal dominant inheritance and no effective treatment is currently available (Cabianca and Gabellini, 2010). FSHD typically arises with a reduction of facial and shoulder girdle muscle mass. The disease may extend to abdominal and pelvic girdle muscles impairing the ability to walk. Although FSHD is primarily a disease of skeletal muscle, up to 75% of FSHD patients also present vascular defects (Fitzsimons et al., 1987; Osborne et al., 2007; Padberg et al., 1995).

FSHD is characterized by extreme variability. Asymmetric distribution of muscle wasting and gender differences in the severity of the phenotype are often observed (Tonini et al., 2004; Zatz et al., 1998). Moreover, the onset, the progression and the severity of the phenotype, even between individuals carrying the same genetic mutation, differ dramatically among patients. Notably, several monozygotic-twin discordances for FSHD have been reported (Griggs et al., 1995; Hsu et al., 1997; Tawil et al., 1993; Tupler et al., 1998). Although the molecular basis of this heterogeneity is not fully understood, an increasing body of evidence suggests that it derives from the interplay of complex genetic and epigenetic events (Neguembor and Gabellini, 2010).

FSHD is associated with reduction in the copy number of a macrosatellite repeat, called D4Z4, located at the subtelomeric region of chromosome 4 long arm, in 4q35 (Wijmenga et al., 1992). In healthy individuals, the number of repeats varies between 11 and 100, while FSHD patients carry 1 to 10 repeats (van Deutekom et al., 1993). The reduction in D4Z4 copy number causes a Polycomb/Trithorax epigenetic switch leading to the over-expression of several genes within the FSHD region (Cabianca et al., 2012). The unusual nature of the mutation that causes FSHD and its complex effect on chromatin surrounding the 4q35 region makes it highly unlikely that the root cause of the disease can be attributed to a single gene. Since expression of multiple

genes is affected, the molecular pathogenesis of FSHD has been challenging to untangle, and as yet no therapy is available for FSHD patients. The two most important FSHD candidate genes are the D4Z4 repeat gene *double homeobox 4* (*DUX4*) (Lemmers et al., 2010; Snider et al., 2009; Snider et al., 2010) and the proximal gene *FSHD Region Gene 1* (*FRG1*) (Gabellini et al., 2002). *DUX4* transgenic mice have been recently described (Krom et al., 2013). Despite they display a *DUX4* expression pattern and an alteration of DUX4 target genes similar to FSHD patients, ~~a lot of effort,~~ *DUX4* transgenic mice do not display any obvious muscle phenotype (Krom, et al., 2013)~~showing muscle pathology are currently not available~~. On the contrary, *FRG1* transgenic mice develop muscular dystrophy (Gabellini et al., 2006). In addition, studies conducted in *X. laevis* and *C. elegans* revealed that *frg1* is required for normal muscle development and its over-expression causes muscle defects and vascular abnormalities correlated with the clinical findings from FSHD patients (Hanel et al., 2009; Liu et al., 2010; Wuebbles et al., 2009).

FRG1 is a dynamic nuclear and cytoplasmic shuttling protein that, in skeletal muscle, is also localized to the sarcomere (Hanel et al., 2011). Interestingly, over-expressed FRG1 is almost completely nuclear and is localized in nucleoli, Cajal bodies, and actively transcribed chromatin (Sun et al., 2011; van Koningsbruggen et al., 2004). Although, it has been associated with RNA biology (Gabellini, et al., 2006; Sun, et al., 2011; van Koningsbruggen, et al., 2004; van Koningsbruggen et al., 2007), the molecular and cellular mechanism that follows *FRG1* over-expression leading to muscular defects is currently unknown.

Here, we show that FRG1 directly binds to Suppressor of variegation 4-20 homolog 1 (Suv4-20h1), a histone methyltransferase previously involved in constitutive heterochromatin formation (Benetti et al., 2007; Gonzalo et al., 2005; Schotta et al., 2004). Our data indicate that Suv4-20h1 is required for myogenic differentiation and that FRG1 over-expression interferes with its function. Finally, we show that *EP300 interacting inhibitor of differentiation 3* (*Eid3*) is an FRG1/Suv4-20h1 epigenetic target. Based on these findings, we propose that FRG1 and Suv4-20h1 are novel epigenetic regulators of muscle differentiation.

RESULTS

FRG1 directly interacts with the histone methyltransferase SUV4-20H1.

The molecular mechanism that follows *FRG1* over-expression is currently unknown. To address this, we performed an unbiased yeast two-hybrid screening to identify potential interaction partners. In accordance with van Koningsbruggen et al. 2007, we identified Karyopherin alpha 2 (KPNA2) as first interactor with 30% of positive clones. The second interactor identified (18.8% of positive clones) ~~Among the positive clones, we isolated a clone~~ corresponded~~ing~~ to the C-terminus region (517-885) of human Suppressor of variegation 4-20 homolog 1 (SUV4-20H1), a histone methyltransferase responsible for the di- and tri-methylation of Lysine 20 of Histone 4 (H4K20me2 and H4K20me3) (Schotta, et al., 2004). These epigenetic modifications play a crucial role in the control of repressive heterochromatin (Schotta, et al., 2004). Interestingly, there are several indications that H4K20me3 is implicated in muscle differentiation (Biron et al., 2004; Terranova et al., 2005; Tsang et al., 2010). The levels of H4K20me3 dramatically increase during muscle differentiation (Biron, et al., 2004; Terranova, et al., 2005) and it has been suggested that this could act as a switch in the myogenic program (Tsang, et al., 2010). Therefore, SUV4-20H1 appeared as an interesting FRG1 interacting partner that could provide a molecular clue in the myogenic defects associated with *FRG1* over-expression.

~~Unfortunately, antibodies functioning in co immunoprecipitation with endogenous FRG1 and Suv4-20h1 are not available. Moreover, Suv4-20h1 is tightly bound to chromatin and very high salt is required to quantitatively extract it . Accordingly, endogenous interaction between Suv4-20h1 and other proteins has never been reported . For these reasons,~~ We first investigated the FRG1/SUV4-20H1 interaction *in vivo* by co-immunoprecipitation and found that endogenous SUV4-20H1 interacts with over-expressed FRG1 (Figure 1A). To further confirm this interaction, we used co-immunoprecipitation with epitope-tagged proteins ~~to confirm FRG1/SUV4-20H1 interaction *in vivo*~~ and showed that FRG1 binds to both human and murine Suv4-20h1 *in vivo*

(Supplementary Figure S1A–B). ~~Interestingly, we found that FRG1 tends to co-immunoprecipitate more abundantly than human or murine Suv4-20h1. Although co-immunoprecipitation assays cannot define the stoichiometry of an interaction, it is possible that multimers of FRG1 could bind to Suv4-20h1 since it has been recently shown that FRG1 forms dimers and tetramers to establish protein-protein interactions .~~ Next, we performed *in-vitro* pull-down assays using purified, recombinant full-length proteins as well as the C-terminus region of Suv4-20h1 to validate our yeast two-hybrid results. Accordingly, we established that FRG1 and Suv4-20h1 interact in a direct manner and that the binding occurs through the C-terminal region of the protein (Figure 1B~~C~~). In particular, from a panel of truncated forms of Suv4-20h1 (Figure 1C~~D~~), we found that the Suv4-20h1(509-630) region was sufficient for FRG1 binding *in vitro* (Figure 1D~~E~~). Notably, we also showed by co-immunoprecipitation that the Suv4-20h1(509-630) region is sufficient to interact with FRG1 *in vivo* (Figure 1E~~F~~).

We then sought to investigate the FRG1 and SUV4-20H1 interaction at the cellular level. Figure 2 shows that, when expressed singularly, the two proteins displayed distinct localizations in line with previous reports (Hanel, et al., 2011; Schotta, et al., 2004; van Koningsbruggen, et al., 2004; van Koningsbruggen, et al., 2007). As previously shown, SUV4-20H1 was localized in DAPI-dense, heterochromatic regions (Schotta, et al., 2004), while FRG1 was broadly distributed in the nucleus with nucleolar enrichment (Hanel, et al., 2011; van Koningsbruggen, et al., 2004; van Koningsbruggen, et al., 2007). Strikingly, in cells over-expressing FRG1, SUV4-20H1 was de-localized from heterochromatin, showed a wider nucleoplasmic distribution and co-localized with FRG1 (Figure 2A). Several controls support the specificity of these results. Firstly, the result was independent from the position or the nature of the tag fused to SUV4-20H1 (data not shown). Secondly, the localization of a SUV4-20H1 isoform lacking the FRG1 binding domain (SUV4-20H1.2) (Tsang, et al., 2010), was not altered in cells over-expressing FRG1 (Figure 2B). Thirdly, SUV4-20H2, a heterochromatin enriched histone methyltransferase that shares the enzymatic

activity of SUV4-20H1 (Schotta, et al., 2004), was unaffected by FRG1 over-expression (Figure 2C).

Collectively, our results suggest that *FRG1* over-expression specifically alters SUV4-20H1 sub-nuclear distribution titrating it away from some target loci.

The functional interaction between FRG1 and SUV4-20H1 is evolutionarily conserved in *Drosophila*.

Since the *Drosophila* homolog of SUV4-20H1, dSuv4-20, was identified as a dominant suppressor of position effect variegation (PEV) (Schotta, et al., 2004), we asked whether dFRG1, the *Drosophila* homolog of FRG1, could also have an effect on PEV. While no d*FRG1* mutant is available, we took advantage of available d*FRG1* RNAi flies (Vienna Drosophila RNAi Stock center). As previously done (Schotta, et al., 2004), PEV analyses were conducted on the $T(2;3)Sb^{V}$ background where the dominant negative marker *Stubble* (Sb^{V}), which gives rise to short bristles, is translocated close to pericentric heterochromatin being hence subjected to PEV-dependent silencing (Moore et al., 1983; Sinclair et al., 1983). When crossed into the $T(2;3)Sb^{v}$ background, $Suv4\text{-}20^{BG00814}$ mutation leads to de-repression of the dominant *Stubble* allele (Figure S~~1~~2A; Fisher exact test: $p<0.0001$, n=400 from 20 flies), as previously reported (Schotta, et al., 2004). Conversely, $UAS\text{-}FRG1^{RNAi}$ ($FRG1^{RNAi}$) flies showed stronger silencing of pericentric heterochromatin compared to the control (Figure S2~~1~~A; Fisher exact test: $p<0.0001$, n=400 from 20 flies). To investigate the molecular mechanism, we monitored the levels of the dSuv4-20-associated repressive histone mark H4K20me3 on chromosomal spreads from salivary glands. As previously reported (Schotta, et al., 2004), $Suv4\text{-}20^{BG00814}$ mutation lead to a decrease in H4K20me3 compared to controls (Figure S~~1~~2C-D; unpaired t test: $p<0.0001$, n=5). On the contrary, $FRG1^{RNAi}$ flies displayed increased H4K20me3 levels (Figure S~~1~~2C-D; unpaired t test: $p<0.0001$, n=5). These data indicate that the interaction between FRG1 and SUV4-20H1 is evolutionarily conserved and suggest that the regulation of Suv4-20 function is part of the normal FRG1 activity in *Drosophila*.

FRG1 over-expression or _Suv4-20h1_ knockdown inhibits myogenic differentiation of C2C12 muscle cells.

The regulation of H4K20 methylation has been implicated in muscle differentiation (Biron, et al., 2004; Terranova, et al., 2005). Moreover, over-expression of Suv4-20h proteins can enhance myogenic differentiation (Tsang, et al., 2010). Based on our results, we reasoned that over-expression of *FRG1* could interfere with Suv4-20h1 function. To verify this hypothesis, we investigated the myogenic differentiation of C2C12 muscle cells over-expressing *FRG1* or knockdown for *Suv4-20h1*. Both *FRG1* over-expression and *Suv4-20h1* knockdown, using three independent shRNAs, were able to reduce the myogenic differentiation ability of C2C12 cells (Figure 3A–D; paired t test: $p=0.0067$, $n=3$ and one-way Anova test: $p<0.0001$, $n=3$ respectively). Noteworthy, low levels of *FRG1* over-expression and a partial *Suv4-20h1* knockdown were sufficient to observe this phenotype (Figure 3E–F). These results indicate that appropriate expression levels of both proteins are required for muscle differentiation in C2C12 cells.

Our data suggest that the interference with Suv4-20h1 function is an important mechanism through which *FRG1* over-expression affects myogenic differentiation. Based on this, we reasoned that over-expression of *SUV4-20H1* in *FRG1* over-expressing cells could rescue their myogenic defect. Since the constitutive over-expression of *SUV4-20H1* is not well tolerated by C2C12 myoblasts (Tsang, et al., 2010), we used an inducible SUV4-20H1_ERα fusion, allowing the translocation of the protein to the nucleus upon 4-hydroxytamoxifen (4-OHT) treatment. By performing differentiation experiments, we observed a partial but significant amelioration of the phenotype in *SUV4-20H1_ERα/FRG1* over-expressing cells treated with 4-OHT compared to control cell ~~line~~s (*FRG1*) (Figure 4A-C; two way Anova test, $p= 0.0406$; $n=3$). Overall, these results indicate that *FRG1* over-expression inhibits muscle differentiation at least in part by interfering with Suv4-20h1 function.

Muscle-specific *Suv4-20h* knockout mice develop muscular dystrophy signs.

Suv4-20h1 and the related enzyme Suv4-20h2 share functional redundancy in muscle (Schotta et al., 2008). To further investigate the role of Suv4-20h on muscle biology, we crossed *Suv4-20h1*$^{-/flox}$*_Suv4-20h2*$^{-/-}$ mice with transgenic mice expressing the *cre recombinase* gene selectively in the skeletal muscle to obtain *Suv4-20h1_Suv4-20h2* muscle-specific double knockout (*mDKO*) mice. Unfortunately, we obtained only a partial excision of the *Suv4-20h1*^{flox} allele and a partial reduction of *Suv4-20h1* expression (~~Supplementary~~ Figure 5~~S2~~A-B), resulting in significant residual H4K20me3 levels in the skeletal muscle (~~Supplementary~~ Figure 5~~S2~~C). Nevertheless, *mDKO* mice displayed several signs of muscular dystrophy, including necrosis (Figure 5D~~A~~–~~E~~~~B~~; Mann-Whitney test: p=0.0079, n=5) and an increased number of centrally-nucleated myofibers (Figure 5~~A~~D and 5F~~C~~; Mann-Whitney test: p=0.0079, n=5). Collectively, these results suggest that Suv4-20h1 activity plays a relevant role in muscle biology and the interference with Suv4-20h1 function might contribute to the muscular dystrophy signs associated with *FRG1* over-expression.

The novel inhibitor of differentiation *Eid3* is an FRG1/Suv4-20h1 target involved in the myogenic defects caused by FRG1 over-expression.

Based on our results, we hypothesized that FRG1 could repress myogenesis at least in part by binding to Suv4-20h1 and interfering with its function. While Suv4-20h1 has been mainly associated with establishment and maintenance of constitutive heterochromatin, in particular at pericentric regions (Schotta, et al., 2004), we found no evidence of global changes in H4K20me3 in *FRG1* over-expressing ~~cells (data not shown)~~and a slight reduction in *Suv4-20h1* knock-down cells compared to controls (Supplementary Figure S3). This result is expected since Suv4-20h2 is able to compensate for the lack of Suv4-20h1 in pericentric heterochromatin regions that constitute the major target of Suv4-20h proteins (Schotta, et al., 2008). Given this, we hypothesized that FRG1 could act at a gene-specific level by hindering the recruitment of Suv4-20h1 to a subset of its targets preventing their silencing. For example, the over-expression of FRG1 could prevent the silencing of

"myogenic inhibitors" by Suv4-20h1. To test our hypothesis, we focused on the differential expression of differentiation inhibitor genes in skeletal muscles from *FRG1* mice compared to *WT* controls (Xynos et al., 2013)~~(Xynos et al, submitted)~~. Among the differentially expressed genes, DNA microarray and qRT-PCR validation (Supplementary Figure S4~~3~~) identified the up-regulation of *EP300 interacting inhibitor of differentiation 3* (*Eid3*) (Bavner et al., 2005). Despite its name, no information is available toward the biological function of Eid3. To understand if *Eid3* could play a role in myogenic differentiation, we first analysed its expression levels in both primary and C2C12 muscle cells and we found that *Eid3* is normally silenced during myogenic differentiation (Figure 6A-B; unpaired t test: $p<0.0001$, n=3 and one sample t test: $p=0.0052$, n=3 respectively). To assess whether its repression is required for muscle differentiation, we generated stable *Eid3* over-expressing C2C12 cells (p*H-Eid3*) where we observed that *Eid3* over-expression reduces myogenic differentiation compared to control cells ~~line~~ (p*FH*) (Figure 6C-E; paired t test: $p=0.0057$, n=3), thus suggesting that Eid3 acts as an inhibitor of muscle differentiation.

Interestingly, we found that *Eid3* expression remains significantly higher in muscles and C2C12 cells over-expressing *FRG1* (Figure 7A-B; paired t test: $p=0.0039$, n=5 and one sample t test: $p=0.0025$, n=4 respectively). Importantly, increased *Eid3* expression was already present in young, pre-dystrophic *FRG1* mice indicating that altered *Eid3* expression is not simply secondary to muscle wasting (Figure 7A; paired t test: $p=0.0039$, n=5). Moreover, *Eid3* over-expression was significantly higher in muscles that are highly affected in *FRG1* mice (*vastus lateralis*) compared to mildly affected muscles (*biceps brachii*), suggesting that de-regulation of *Eid3* expression correlates with the severity of the disease in different muscles (Figure 7C; paired t test: $p=0.0086$, n=3). *Eid3* expression was also significantly increased in muscles from *mDKO* mice and in C2C12 muscle cells knockdown for *Suv4-20h1* (Figure 7D-E; unpaired t test: $p=0.0019$, n=5 and one sample t test: $p=0.0039$, n=4 respectively), suggesting that FRG1 over-expression affects *Eid3* expression through Suv4-20h1. Intriguingly, we observed that *EID3* expression was significantly up-regulated in biopsies of FSHD patients compared to healthy subjects (Figure 7F; one-way Anova test:

p=0.00290485, n=73 4); while *EID3* levels were normal in patients affected by other types of Becker muscular dystrophy (Figure 7F, n=8). Similar results were obtained for *FRG1* (Figure 7G, one-way Anova test: p=0.0013, n=7-8), while of *SUV4-20H1* and *β-glucuronidase* (*GUS*), a gene with stable expression in FSHD (Krom et al., 2012), were not altered in FSHD patients compared to controls (Supplementary Figure S5), suggesting that *FRG1* and *EID3* up-regulation areis not a general feature of muscular dystrophies. Notably, *EID3* up-regulation in FSHD patients was significantly correlated with increased *FRG1* levels (Figure 7H, Pearson test: R^2=0.6611,; p<0.0001=0.0213, n=227).

To determine if the aberrant *Eid3* up-regulation could be associated to a lack of epigenetic silencing by Suv4-20h1, we investigated the levels of the Suv4-20h1-associated repressive histone mark, H4K20me3, at the *Eid3* promoter. Chromatin immunoprecipitation revealed that H4K20me3 levels were significantly reduced at the *Eid3* genomic regions spanning -6 to -2 kb from the transcription start site, both in *FRG1* over-expressing and *Suv4-20h1* knockdown C2C12 muscle cells (Figure 7IG JH; two-way Anova test: p=0.0099 and p=0.0043 respectively). These data suggest that *FRG1* over-expression might interfere with Suv4-20h1-dependent H4K20 trimethylation of the *Eid3* promoter, potentially resulting in its aberrant up-regulation.

To investigate whether the lack of repression of *Eid3* plays a role in the *FRG1*-associated phenotype, we down-regulated *Eid3* expression in C2C12 cells over-expressing *FRG1*. Down-regulation of *Eid3* was able to significantly rescue the myogenic defect of *FRG1* over-expressing cells compared to controls (Figure 8A-C; paired t test: p=0.0009, n=5). Collectively, our results suggest that the over-expression of *FRG1* interferes with the repressive activity of Suv4-20h1 leading to aberrant *Eid3* up-regulation and myogenic defects.

DISCUSSION

In this study, we focused on the largely unexplored role of FRG1 in muscle biology. We have recognized Suv4-20h1 as a direct FRG1 interactor and revealed that it is aberrantly localized upon *FRG1* over-expression, suggesting that over-expression of FRG1 could interfere with Suv4-20h1 function. Accordingly, the lack of *Suv4-20h1* reproduced phenotypes similar to the *FRG1* over-expression while its over-expression ameliorates *FRG1*-associated myogenic defects. Altogether, these results suggest that the interference with Suv4-20h1 activity might play a relevant role in the myogenic defects associated to *FRG1* over-expression. Notably, similar mechanisms might govern differentiation in other contexts. For example, it was recently reported that differentiation of postnatal spermatogonial progenitor cells (SPCs) is regulated by physical interaction and altered localization of the essential factors Sall4 and Plzf (Hobbs et al., 2012). Similarly to FRG1, Plzf is localized to euchromatic regions and nuclear speckles (Melnick et al., 2000). On the contrary, Sall4 is associated with DAPI-dense pericentric heterochromatin like Suv4-20h1 (Sakaki-Yumoto et al., 2006; Yamashita et al., 2007). When its expression increases in postnatal testis, Plzf binds Sall4 sequestering it away from heterochromatin. This allows the expression of *Sall1*, a gene repressed by Sall4, and the inhibition of SPCs differentiation. Thus, it is tempting to speculate that the regulation of differentiation through altered localization of an heterochromatin-associated protein could be a more general mechanism used by other proteins.

Suv4-20h1 has been traditionally considered to be involved in the structural maintenance of constitutive heterochromatin (Benetti, et al., 2007; Gonzalo, et al., 2005; Schotta, et al., 2004). Instead, our data show that Suv4-20h1 plays a relevant role in muscle biology and uncover a novel function for Suv4-20h1 as a gene-specific repressor required for myogenic differentiation. In particular, our results suggest that *Eid3* (Bavner, et al., 2005) is a novel inhibitor of differentiation and a Suv4-20h1 target. We found that *Eid3* expression is normally silenced upon induction of myogenic differentiation, but its silencing fails in C2C12 muscle cells over-expressing *FRG1* or

knocked-down for *Suv4-20h1*. Based on our results, we propose that FRG1 over-expression might sequester Suv4-20h1 away from its epigenetic targets leading to their inappropriate de-repression (Figure 8D). Accordingly, we found that over-expression of *FRG1* or *Suv4-20h1* knockdown are both associated to an epigenetic de-regulation of the Suv4-20h1 enzymatic product, the repressive mark H4K20me3, at the *Eid3* promoter.

Despite its extensive study, FSHD pathogenesis remains unclear and controversial. All current models predict that deletion of D4Z4 repeats results in the de-regulation of a candidate gene(s), located in the FSHD region, leading to disease (Cabianca and Gabellini, 2010; van der Maarel et al., 2011). While the two most accepted FSHD candidate genes are *DUX4* and *FRG1*, the molecular and cellular mechanism following their de-regulation and finally causing the disease remains elusive. Furthermore, FSHD is characterized by an extreme variability in disease onset, progression and severity. This heterogeneity in disease manifestation could reflect heterogeneity in gene expression of FSHD candidate gene(s). An interesting possibility, therefore, is that the complexity of FSHD could be explained envisaging that the epigenetic alteration of *DUX4*, *FRG1* and other potential genes could collaborate to determine the final phenotype. In this context, it is relevant to investigate the biological role of these players and address how each could contribute to the different aspects of the disease such as the muscle differentiation defects described in FSHD (Barro et al., 2005; Celegato et al., 2006; Tupler et al., 1999; Winokur, Barrett, et al., 2003; Winokur, Chen, et al., 2003). We found that *Eid3* is up-regulated in affected muscles of *FRG1* over-expressing or *Suv4-20h* knockout mice and *EID3* levels are inappropriately increased in biopsies of FSHD patients. Our results suggest that *FRG1* and *EID3* up-regulation are~~is~~ not a general feature of muscular dystrophies but are~~is~~ selectively found in FSHD patients when compared to other muscular dystrophy patients. Importantly, we have found that *Eid3* over-expression causes muscle differentiation defects while its knockdown rescues the myogenic defects in *FRG1* over-expressing cells. Overall, these data promote *Eid3* a novel myogenic inhibitor that might explain, at least in part, the muscle differentiation defects associated to *FRG1* over-expression.

MATERIALS AND METHODS

Ethics Statement

All procedures involving human samples were approved by the Fondazione San Raffaele del Monte Tabor Ethical Committee. All animal procedures were approved by the Institutional Animal Care and Use Committee of the Fondazione San Raffaele del Monte Tabor and were communicated to the Ministry of Health and local authorities according to Italian law.

Yeast Two-Hybrid Screening

MATCHMAKER two-hybrid system 3 (Clontech) was used for this study. DNA-BD/*FRG1* and AD/HeLa cDNA plasmid library ($3.5x10^6$ independent clones) were co-transformed in yeast and plated onto high stringency SD/–Ade/–His/–Leu/–Trp/3-AT/X-a-Gal plates. A total of $20x10^6$ clones were screened corresponding to a ~6 fold coverage of the HeLa cDNA library. AD/library plasmids were isolated from positive clones, rescued via transformation of *E. coli* and sequenced. In accordance with van Koningsbruggen et al. 2007, we identified Karyopherin alpha 2 (KPNA2) as first interactor with 30% of positive clones. SUV4-20H1 was the second protein identified with 18.8% of positive clones.

Constructs and cloning procedures

All primers employed for cloning are listed in Supplementary Table I. PCR amplifications were performed with *Pfx50 DNA polymerase* (Invitrogen) or GoTaq polymerase (Promega). PCR products were digested with the restriction enzymes (Takara) listed in Supplementary Table I and ligated into the respective destination plasmid with *T4 ligase* (Fermentas). p*CMV-HA* and p*CMV-Myc* (Clontech) were employed for mammalian transient expression, while p*RSET-A* (Invitrogen) and p*GEXT2T* (GE Healthcare) for protein production in *E. coli.* For p*CMV-myc-FRG1*, *FRG1*

coding sequence was excised with *PstI* from p*GBKT7-FRG1,* blunted with *T4 DNA polymerase* (Fermentas) and then digested with *SfiI* to release the insert. p*CMV-myc* (Clontech) was digested with *XhoI*, blunted with *Klenow Fragment of DNA polymerase* (Fermentas) and digested with *SfiI*. p*DEST15GW-Suv4-20h1*, p*GEX-6P1GW-Suv4-20h1(385-874aa)* and p*EGFP-N1-Suv4-20h1* were previously described (Schotta, et al., 2004). p*LKO.1* lentiviral vectors expressing control shRNA or specific shRNAs for *Suv4-20h1* and packaging constructs were purchased from Open Biosystems. p*BABE-SUV4-20H1_ERα* plasmid was a kind gift of Dr. Holger Bierhoff (German Cancer Research Center, Heidelberg, Germany). For p*IRESneo3-HA-Eid3* (p*H-Eid3*), *Eid3* was first amplified from C2C12 cDNA with the primers listed in Supplementary Table I and cloned into p*CMV-HA* (Clontech). The *HA-Eid3* sequence was then excised with *StuI* and *NotI* and ligated into p*IRESneo3* (Clontech) previously digested with the same enzymes.

Proteins purification

6xHis-FRG1 and GST-Suv4-20h1 proteins were expressed in Rosetta2(DE3)pLys *E.coli* (Novagen). Protein expression was induced at 0.4-0.6 OD with 1mM IPTG (Biosciences) for 3h at 37°C (or 8h at 30°C for GST-Suv4-20h1 full-length). Bacterial pellets were resuspended in PBS and Protease Inhibitor cocktail (PI; Sigma) or in Lysis Buffer (50mM NaH_2PO_4, 250 mM NaCl, pH 8.0, plus PI) for GST- and His-tagged proteins, respectively. Bacteria were lyzed by sonication (Bandelin), incubated by gentle rotation for 15 min at 4°C, after adding TritonX100 (1%; Sigma), and centrifuged at 19.000 rpm at 4°C for 20 min. Supernatants were incubated for 1 h at 4°C in batch with Glutathione-Agarose beads (Sigma) or HIS-Select Nickel Affinity gel beads (Sigma). Beads were packed on a disposable column and washed by gravity flow with 50 beads volumes of PBS-TritonX100 (1%) plus PI or Lysis buffer supplemented with 10mM Imidazole (Fluka), for GST and His-tagged proteins respectively. Proteins were eluted with 50 mM Tris-HCl pH 9.0, 10 mM Reduced L-Glutathione (Sigma) plus PI or 50mM NaH_2PO_4, 250 mM NaCl, 250 mM of Imidazole, pH 8.0 plus PI, for GST and His-tagged proteins respectively. Proteins were dialyzed

overnight at 4°C in dialysis cassettes (Slide-A-Lyzer Dialysis Cassettes; Thermo scientific) in 50 mM Tris-HCl, pH 9.0 or in 50mM NaH_2PO_4, 250 mM NaCl, pH 8.0, for GST- and His-tagged proteins respectively. After dialysis, glycerol was added to His-tagged proteins to a 10% final concentration.

Co-immunoprecipitation assays

For figure 1A, HEK293T cells were transfected with p*CMV-Myc-FRG1*. For figures S1A and S1B, HEK293T cells were co-transfected with p*CMV-HA-SUV4-20H1*/p*CMV-HA-Suv4-20h1(509-630)*/p*CMV-HA* or p*EGFP-N1-Suv4-20h1*/p*EGFP-N3* and p*CMV-Myc-FRG1*/p*CMV-Myc* with Lipofectamine LTX (Invitrogen) according to manufacturer's instructions, plasmids were transfected in a 1:1 ratio. Cells were collected after 36h from transfection. Co-immunoprecipitation (co-IP) assays were performed as described in (van Koningsbruggen, et al., 2007) with -mouse anti-HA clone 16B12 (MMS-101R, Covance), ~~or~~ rabbit anti-GFP (A11122, Molecular Probes), rabbit anti-SUV4-20H1 (LS-C161629, Lifespan Bioscience) or rabbit IgG (#011-000-003, Jackson Immunoresearch). Input (0.1% or 3%) and Bound (20%) fractions of the co-IP were analyzed by SDS-PAGE followed by immunoblotting with the above-mentioned primary antibodies at 1/500 dilution for anti-SUV4-20H1 and 1/1000 dilution anti-HA, anti-GFP and mouse anti-c-Myc clone 9E10 (MMS-150R Covance). ~~and a~~Anti-mouse and anti-rabbit IgG HRP-conjugated ~~secondary antibody~~ (#715-035-150 and #711-035-152, Jackson ImmunoResearch; dilution: 1/20000) secondary antibodies were used.

GST and Histidine pull-down assays

Pull-down assays were performed by incubating, overnight at 4°C, equal molar amounts (10 to 50 picomoles) of GST-tagged with His-tagged proteins in cold CHAPS buffer [50 mM Tris-HCl pH 7.4, 150 mM NaCl, 0.15% CHAPS (3-[(3-Cholamidopropyl) dimethylammonio]-1-propanesulfonate; Fluka) and Protease Inhibitor Cocktail (Sigma) plus 5mM Imidazole for His pull-

downs (van Koningsbruggen, et al., 2007). 20 µl of beads slurry were added and incubated for 1 h at 4°C and then washed 4 times with 1 ml cold CHAPS buffer, one time with 1 ml cold 50 mM Tris-HCl pH 7.4 plus PI and boiled in 50 µl of 1X Laemmli buffer at 95°C for 8 min. Input (1%) and Bound (20%) fractions were analyzed by immunoblotting with mouse anti-GST (G1160, Sigma; dilution: 1/10000) mouse anti-6xHis (#631212, Clontech; dilution: 1/5000,) and anti-mouse IgG HRP-conjugated secondary antibody (#715-035-150, Jackson ImmunoResearch; dilution: 1/20000).

FRG1 and SUV4-20H1 localization analysis

C2C12 cells were seeded on glass coverslips and were co-transfected 24h later with p*CMV-Myc-FRG1* or p*CMV-Myc* and p*EGFP-C1-SUV4-20H1_i1*, p*EGFP-C1-SUV4-20H1_i2*, p*EGFP-C1-SUV4-20H2,* kindly provided by Alan Underhill (University of Alberta, Canada) (Tsang, et al., 2010) or p*EGFP-N3* (Clontech) with Lipofectamine LTX (Invitrogen) according to manufacturer's instructions. Plasmids were transfected in a 1:1 ratio (500ng each). Cells were fixed in 4% paraformaldehyde (Electron Microscopy Science) 36h post transfection. Immunofluorescence was performed with mouse anti-c-Myc clone 9E10 (MMS-150R Covance; dilution 1/5000). Alexa Fluor 555 goat anti-mouse (Molecular Probes, 1/500) was used for secondary detection. Samples were mounted in aqueous medium and acquired at room temperature, using a Deltavision Restoration Microscopy System (Applied Precision) built around an Olympus IX70 microscope equipped with mercury-arc illumination CoolSnap_Hq/ICX285 CCD camera. 0.1µm sections were collected with an Olympus 60X/1.4 NA Plan Apo oil immersion objective lens and deconvolved with SoftWoRx 3.5.0 (Applied Precision) by the constrained iterative algorithm using 10 iterations and standard parameters. Representative pictures of three independent experiments are shown.

***Drosophila* Position Effect Variegation analysis**

Flies were raised at 25°C on K12 Medium (USBiological). All crosses were conducted at 25°C. *Suv4-20*^{BG00814} (Bloomington, stock # 12510), *UAS-FRG1*^{RNAi} (Vienna Drosophila RNAi

Stock center, stock # v23447), w1118 (Bloomington, stock # 3605) and *T(2;3)Sb^V/TM3,Ser* (kindly provided by Sergio Pimpinelli) fly strains were employed for this study. *T(2;3)Sb^V* translocation juxtaposes the *Sb* mutation and the centric heterochromatin of the second chromosome, resulting in a mosaic flies with both *Sb* and normal bristles. Activation of dominant *Sb* results in *Stubble* bristles. For *Stubble* (*Sb^V*) variegation analysis, ten pairs of major dorsal bristles of 20 flies were analyzed assigning a *Sb$^-$* or *Sb$^+$* phenotype to each bristle. The extent of *Sb* variegation was expressed as the mean of *Sb* and WT bristles per strain.

Immunofluorescence on *Drosophila* polytene chromosome spreads

Larval salivary glands were dissected from third-instar larvae grown at 25°C. Immunofluorescence on polytene chromosome spreads were conducted as previously described (Burgio et al., 2008) with rabbit anti-H4K20me3 (ab9053, Abcam; dilution: 1/500). Images were acquired with a Leica DM 4000B microscope and densitometric analysis was performed with LAS AF Software (Leica). Quantification was carried out by calculating the intensity ratio between FITC (H4K20me3) and DAPI channels. Five chromosomal spreads were analyzed per strain.

Cell lines generation, cell culture and differentiation

HEK293T and Phoenix-Eco cells were cultured at 37°C in a 5% CO_2 humidified incubator in DMEM supplemented with 10% FBS and 1% Penicillin/Streptomycin. C2C12 cells were cultured at 37°C in a 5% CO_2, 5% O_2 humidified incubator in DMEM supplemented with 10% FBS and 1% Penicillin/Streptomycin, plus 0.5 µg/µl G418 (Invivogen) for p*FLAG-HA*, p*FLAG-HA-FRG1* and p*HA-Eid3* cells or plus 0.5 µg/ml puromycin (Invivogen) for p*LKO.1* and p*BABEpuro* cells.

p*FH-FRG1* and p*FH* C2C12 cells were previously described (Gabellini, et al., 2006).

p*LKO.1* C2C12 cells expressing the non-silencing shRNA control or shRNAs specific for *Suv4-20h1* were generated by lentiviral transduction of C2C12 cells according to manufacturer's

instructions (Open Biosystems) and maintained as polyclonal populations under puromycin selection.

p*BABE-SUV4-20H1_ERα*/p*FH-FRG1* over-expressing C2C12 cells were generated by retroviral transduction of p*FH-FRG1* myoblasts. Retroviral particles were prepared from Phoenix-Eco cells (a gift from Dr. Gary P. Nolan) following the Nolan Laboratory protocol (http://www.stanford.edu/group/nolan/protocols/pro_helper_dep.html). Transduced cells were subjected to double G418 (0.5 µg/µl) and Puromycin (0.5 µg/ml) selection. Resistant cells were maintained as polyclonal population and grown under constant selection. The translocation of SUV4-20H1_ERα to the nucleus was induced with 500nM 4-hydroxytamoxifen (4-OHT) treatment (H7904, Sigma) for 72h prior to differentiation; 4-OHT was maintained during differentiation.

p*H-Eid3* cells were generated by transfecting C2C12 cells with linearized p*H-Eid3* or p*FH* using Lipofectamine LTX (Invitrogen) according to the manufacturer's instructions, 48h later, 0.5 µg/µl G418 was added to the media. G418-resistant cells were maintained as a pool and grown under constant selection.

Eid3 knock-down/p*FH-FRG1* over-expressing C2C12 cells were generated by transfecting p*FH-FRG1* myoblasts with 50nM siRNAs against *Eid3* (L-046381-01, ON-TARGETplus SMARTpool, Mouse 1700027M21RIK, Thermo Scientific) or non-silencing control (D-001810-10, ON-TARGETplus Non targeting pool, Thermo Scientific) following manufacturer's instructions. Transfections were performed 72h prior to differentiation.

Proteins over-expression and down-regulation were evaluated by immunoblotting with mouse anti-FRG1 (sc-101050, Santa Cruz; dilution 1/500) for p*FH-FRG1*, mouse anti-HA clone 16B12 (MMS-101R, Covance; dilution 1/500) for p*FH-FRG1* and for p*H-Eid3*, rabbit anti-SUV4-20H1 (ab18186, Abcam; dilution 1/1000) for p*LKO.1 Suv4-20h1* knockdown cells, rabbit anti-ERα (sc-543, Santa Cruz, dilution 1/500) for p*BABE-SUV4-20H1_ERα* over-expressing cells, mouse anti-Tubulin (T9026, Sigma; dilution 1/400000) for normalization and anti-mouse or anti-rabbit

IgG HRP-conjugated for secondary detection (#715-035-150 and #711-035-152, Jackson ImmunoResearch; dilution: 1/20000).

Global levels of H4K20me3 in *FRG1* over-expressing and *Suv4-20h1* knock-down cells (myoblasts and myotubes at 3 days of differentiation) were evaluated by immunoblot with rabbit anti-H4-20me3 (kindly provided by Dr. Thomas Jenuwein, dilution 1/300) and rabbit anti-H4 (#62-141-13, Millipore; dilution 1/3000). Histone extracts were obtained following the histone extraction protocol from Abcam (http://www.abcam.com/index.html?pageconfig=resource&rid=11410).

For differentiation experiments, C2C12 cells were plated at confluence in collagen-coated dishes and were differentiated for 3 days in DMEM containing 2% donor horse serum (EuroClone).

For Fusion index quantification, cells were fixed in 4% paraformaldehyde (Electron Microscopy Science) and immunostained with mouse MF20 antibody (Developmental Studies Hybridoma Bank; dilution: ½) followed by Alexa Fluor 488 goat anti-mouse (Molecular Probes, 1/500) and Hoechst (1mg/ml; Sigma; dilution: 1/2000). Samples were visualized at room temperature, using Observer.Z1 (N-Achroplan 10x/0.25 NA Ph1) microscope (Zeiss). Pictures were acquired with a AxioCam MRm camera using its AxioVision Rel. 4.8.2 software by Nikon. Fusion Index analysis was performed with ImageJ by counting the number of nuclei belonging or not to myotubes. Myotubes are considered as myosin positive syncytia containing at least 3 nuclei. A minimum of three independent differentiation experiments were performed, for each experiment at least 6 fields were analyzed, counting at least 1000 nuclei for each cell type.

Human samples.

Muscle biopsies from FSHD and BMD patients and healthy controls were obtained from the Italia Telethon Network of Genetic Biobanks (http://www.biobanknetwork.org)~~Neuromuscular Bank of the Department of Neurosciences, University of Padova, Italy~~. Detailed information regarding the individual samples is provided in Supplementary Table II.

Mouse handling

FRG1-high mice (Gabellini, et al., 2006) and control C57BL/6J littermates were maintained at Charles River (Calco, Italy). To obtain muscle-specific *Suv420h1*$^{-/-}$*_Suv420h2*$^{-/-}$ double knockout mice, *Suv420h1*$^{-/flox}$ and *Suv420h2*$^{-/-}$ mice (Schotta, et al., 2008) were bred with *HSA-cre* mice, in which the *cre recombinase* gene is driven by the *human alpha-skeletal actin* (*HSA*) promoter**.** Mice at 3–18 weeks of age were sacrificed for this study.

Primary muscle cell cultures and Muscle Histology

Cell preparations were obtained by vastus lateralis muscles of four weeks-old males as previously described (Xynos et al., 2011) and were plated on collagen-coated dishes after pre-plating for 1 hour in uncoated dishes. Primary myoblasts were grown in nutrient mixture F-10 Ham (Sigma) supplemented with 20% FBS (Hyclone) and 5ng/ml bFGF (Peprotech) for 1–5 days and differentiated in Dulbecco's modified Eagle medium (DMEM; EuroClone) supplemented with 5% donor horse serum (EuroClone) for 1–2 days. Vastus lateralis and tibialis anterior muscles were dissected, frozen in isopentane cooled in liquid nitrogen and cryosectioned (8-µm thick). Gomori-trichrome staining was performed as previously described (Dubowitz, 1985; Xynos, et al., 2011). For H4K20me3 immunofluorescence, tissue sections were fixed in 4% PFA for 10 min at RT and incubated with rabbit anti-H4K20me3 (ab9053, Abcam; dilution: 1/200). Images were visualized with Imager.M2 (N-Achroplan 20x/0.45 NA) and pictures were acquired with AxioCamMRc5 camera.

Real-time PCR analysis

Total RNA from primary cells and tissues was extracted and treated with DNase 1, using the RNAqueous-4PCR kit (Ambion) and RNeasy Fibrous Tissue Midi or Mini Kit (Qiagen), respectively. cDNA was synthesized using Invitrogen's SuperScript III First-Strand Synthesis Super-Mix. Genomic DNA was extracted with DNeasy Blood & Tissue Kit (Qiagen). qPCRs (for

primers see supplementary table III) were performed with SYBR GreenER qPCR SuperMix Universal (Invitrogen) using Biorad's CFX96 Real-time System. Relative quantification was calculated with CFX Manager Software V.1.6. Validation of the differential expression of genes identified by DNA microarray was performed using TaqMan gene expression assays with custom-made TaqMan array microfluidic cards (Applied Biosystems). Relative quantification was calculated with qBasePLUS V.1.5 using Gapdh, Ppia and 18S rRNA as reference genes.

Chromatin Immunoprecipitation

Cells were briefly washed once in PBS and fixed for 10 minutes in 1% formaldehyde in PBS (from a 37.5% formaldehyde/10% methanol stock). After formaldehyde quenching with Glycine (final concentration 125 mM) for 5 minutes, cells were washed with PBS, harvested by scraping and pelleted. The pellet was lysed in a solution containing 50 mM Hepes-KOH pH 7.5, 140 mM NaCl, 1 mM EDTA, 10% glycerol, 0.5% NP40 and 0.25% Triton X100 for 10 minutes in ice. Nuclei were pelleted and subsequently lysed in a solution containing 10 mM Tris-HCl pH 8.0, 200 mM NaCl, 1 mM EDTA and 0.5 mM EGTA with gentle swirl for 10 minutes. Next, samples were centrifuged and the resulting pellet was resuspended in a solution with 10 mM Tris-HCl pH 8.0, 100 mM NaCl, 1 mM EDTA, 0.5 mM EGTA, 0.1% Na-Deoxycholate and 0.5% N-laurylsarcosine. Chromatin was sheared by sonication using Bioruptor (Diagenode) and Triton X100 was added to lysates at a final concentration of 1%. 10 µg of chromatin were used for each immunoprecipitation and pre-cleared for 3 hours at 4°C with 20 µl of Protein G dynabeads (Invitrogen). Immunoprecipitations were carried out at 4°C overnight with 50 µl of beads previously bound for 3 hours at 4°C with 5 µg of the following antibodies: rabbit anti-H4 (#62-141-13, Millipore), rabbit anti-H4K20me3 (pAb-057-050, Diagenode) and whole molecule rabbit IgG (#011-000-003, Jackson Immunoresearch). Immunoprecipitated chromatin was washed extensively with a solution containing 50 mM Hepes-KOH pH 7.6, 500 mM LiCl, 1 mM EDTA, 1% NP-40 and 0.7% Na-Deoxycholate, and protein–DNA cross-links were reverted by heating at 65°C overnight

in TE buffer with 2% SDS. DNA was purified with QIAquick PCR Purification Kit (Qiagen) and qPCRs were performed using a custom-made ChampionChIP PCR Array (SABiosciences) in Applied Biosystems ViiA 7 Real-Time PCR System.

Statistical analysis

All statistical analyses were two-tailed tests and performed using GraphPad Prism version 5.0a (GraphPad Software, San Diego, USA). The type of statistical test, p value, number of independent experiments, mean and standard error of the mean are provided for each data set in the corresponding figure legends.

ACKNOWLEDGEMENTS

We thank G. Cossu, T. Jenuwein and J. Teodoro for helpful discussions. We are grateful to H. Bierhoff for *SUV4-20H-ER* plasmids and D.A. Underhill for *SUV4-20H* isoforms plasmids. C. Covino and M. Ascagni (San Raffaele Alembic BioImaging Center) are acknowledged for their excellent technical assistance. Maria Victoria Neguembor conducted this study as partial fulfilment of her PhD in Molecular Medicine, Program in Cellular and Molecular Biology, San Raffaele University, Milan, Italy. Davide Gabellini is a Dulbecco Telethon Institute Assistant Scientist.

FUNDING

This work was supported by the European Research Council [grant number 204279], the Italian Epigenomics Flagship Project, the Italian Ministry of Health [grant number GR-2008-1134796], the Italian Telethon Foundation [grant number S05001TELA] and the FSHD Global Research Foundation.

REFERENCES

Barro, M., Carnac, G., Flavier, S., et al. (2005). Myoblasts from affected and non-affected FSHD muscles exhibit morphological differentiation defects. J Cell Mol Med, *14*, 275-289.

Bavner, A., Matthews, J., Sanyal, S., et al. (2005). EID3 is a novel EID family member and an inhibitor of CBP-dependent co-activation. Nucleic Acids Res, *33*, 3561-3569.

Benetti, R., Gonzalo, S., Jaco, I., et al. (2007). Suv4-20h deficiency results in telomere elongation and derepression of telomere recombination. J Cell Biol, *178*, 925-936.

Biron, V. L., McManus, K. J., Hu, N., et al. (2004). Distinct dynamics and distribution of histone methyl-lysine derivatives in mouse development. Dev Biol, *276*, 337-351.

Burgio, G., La Rocca, G., Sala, A., et al. (2008). Genetic identification of a network of factors that functionally interact with the nucleosome remodeling ATPase ISWI. PLoS Genet, *4*, e1000089.

Cabianca, D. S., Casa, V., Bodega, B., et al. (2012). A long ncRNA links copy number variation to a polycomb/trithorax epigenetic switch in FSHD muscular dystrophy. Cell, *149*, 819-831.

Cabianca, D. S., and Gabellini, D. (2010). The cell biology of disease: FSHD: copy number variations on the theme of muscular dystrophy. J Cell Biol, *191*, 1049-1060.

Celegato, B., Capitanio, D., Pescatori, M., et al. (2006). Parallel protein and transcript profiles of FSHD patient muscles correlate to the D4Z4 arrangement and reveal a common impairment of slow to fast fibre differentiation and a general deregulation of MyoD-dependent genes. Proteomics, *6*, 5303-5321.

Dubowitz, V. (1985). Muscle biopsy: A practical approach. London: Bailliere Tindall.

Fitzsimons, R. B., Gurwin, E. B., and Bird, A. C. (1987). Retinal vascular abnormalities in facioscapulohumeral muscular dystrophy. A general association with genetic and therapeutic implications. Brain, *110 (Pt 3)*, 631-648.

Gabellini, D., D'Antona, G., Moggio, M., et al. (2006). Facioscapulohumeral muscular dystrophy in mice overexpressing FRG1. Nature, *439*, 973-977.

Gabellini, D., Green, M. R., and Tupler, R. (2002). Inappropriate gene activation in FSHD: a repressor complex binds a chromosomal repeat deleted in dystrophic muscle. Cell, *110*, 339-348.

Gonzalo, S., Garcia-Cao, M., Fraga, M. F., et al. (2005). Role of the RB1 family in stabilizing histone methylation at constitutive heterochromatin. Nat Cell Biol, *7*, 420-428.

Griggs, R. C., Tawil, R., McDermott, M., et al. (1995). Monozygotic twins with facioscapulohumeral dystrophy (FSHD): implications for genotype/phenotype correlation. FSH-DY Group. Muscle Nerve, *2*, S50-55.

Hanel, M. L., Sun, C. Y., Jones, T. I., et al. (2011). Facioscapulohumeral muscular dystrophy (FSHD) region gene 1 (FRG1) is a dynamic nuclear and sarcomeric protein. Differentiation, *81*, 107-118.

Hanel, M. L., Wuebbles, R. D., and Jones, P. L. (2009). Muscular dystrophy candidate gene FRG1 is critical for muscle development. Dev Dyn, *238*, 1502-1512.

Hobbs, R. M., Fagoonee, S., Papa, A., et al. (2012). Functional antagonism between Sall4 and Plzf defines germline progenitors. Cell stem cell, *10*, 284-298.

Hsu, Y. D., Kao, M. C., Shyu, W. C., et al. (1997). Application of chromosome 4q35-qter marker (pFR-1) for DNA rearrangement of facioscapulohumeral muscular dystrophy patients in Taiwan. J Neurol Sci, *149*, 73-79.

Krom, Y. D., Dumonceaux, J., Mamchaoui, K., et al. (2012). Generation of isogenic D4Z4 contracted and noncontracted immortal muscle cell clones from a mosaic patient: a cellular model for FSHD. The American journal of pathology, *181*, 1387-1401.

Krom, Y. D., Thijssen, P. E., Young, J. M., et al. (2013). Intrinsic Epigenetic Regulation of the D4Z4 Macrosatellite Repeat in a Transgenic Mouse Model for FSHD. PLoS Genet, *9*, e1003415.

Lemmers, R. J., van der Vliet, P. J., Klooster, R., et al. (2010). A unifying genetic model for facioscapulohumeral muscular dystrophy. Science, *329*, 1650-1653.

Liu, Q., Jones, T. I., Tang, V. W., et al. (2010). Facioscapulohumeral muscular dystrophy region gene-1 (FRG-1) is an actin-bundling protein associated with muscle-attachment sites. J Cell Sci, *123*, 1116-1123.

Melnick, A., Ahmad, K. F., Arai, S., et al. (2000). In-depth mutational analysis of the promyelocytic leukemia zinc finger BTB/POZ domain reveals motifs and residues required for biological and transcriptional functions. Molecular and cellular biology, *20*, 6550-6567.

Moore, G. D., Sinclair, D. A., and Grigliatti, T. A. (1983). Histone Gene Multiplicity and Position Effect Variegation in DROSOPHILA MELANOGASTER. Genetics, *105*, 327-344.

Neguembor, M. V., and Gabellini, D. (2010). In junk we trust: repetitive DNA, epigenetics and facioscapulohumeral muscular dystrophy. Epigenomics, *2*, 271-287.

Osborne, R. J., Welle, S., Venance, S. L., et al. (2007). Expression profile of FSHD supports a link between retinal vasculopathy and muscular dystrophy. Neurology, *68*, 569-577.

Padberg, G. W., Brouwer, O. F., de Keizer, R. J., et al. (1995). On the significance of retinal vascular disease and hearing loss in facioscapulohumeral muscular dystrophy. Muscle Nerve, *2*, S73-80.

Sakaki-Yumoto, M., Kobayashi, C., Sato, A., et al. (2006). The murine homolog of SALL4, a causative gene in Okihiro syndrome, is essential for embryonic stem cell proliferation, and cooperates with Sall1 in anorectal, heart, brain and kidney development. Development, *133*, 3005-3013.

Schotta, G., Lachner, M., Sarma, K., et al. (2004). A silencing pathway to induce H3-K9 and H4-K20 trimethylation at constitutive heterochromatin. Genes Dev, *18*, 1251-1262.

Schotta, G., Sengupta, R., Kubicek, S., et al. (2008). A chromatin-wide transition to H4K20 monomethylation impairs genome integrity and programmed DNA rearrangements in the mouse. Genes Dev, *22*, 2048-2061.

Sinclair, D., Mottus, R., and Grigliatti, T. A. (1983). Genes which suppress position-effect variegation in Drosophila melanogaster are clustered. Mol Gen Genet, *191*, 326-333.

Snider, L., Asawachaicharn, A., Tyler, A. E., et al. (2009). RNA transcripts, miRNA-sized fragments and proteins produced from D4Z4 units: new candidates for the pathophysiology of facioscapulohumeral dystrophy. Hum Mol Genet, *18*, 2414-2430.

Snider, L., Geng, L. N., Lemmers, R. J., et al. (2010). Facioscapulohumeral dystrophy: incomplete suppression of a retrotransposed gene. PLoS Genet, *6*, e1001181.

Sun, C. Y., van Koningsbruggen, S., Long, S. W., et al. (2011). Facioscapulohumeral Muscular Dystrophy Region Gene 1 Is a Dynamic RNA-Associated and Actin-Bundling Protein. J Mol Biol, *411*, 397-416.

Tawil, R., Storvick, D., Feasby, T. E., et al. (1993). Extreme variability of expression in monozygotic twins with FSH muscular dystrophy. Neurology, *43*, 345-348.

Terranova, R., Sauer, S., Merkenschlager, M., et al. (2005). The reorganisation of constitutive heterochromatin in differentiating muscle requires HDAC activity. Exp Cell Res, *310*, 344-356.

Tonini, M. M., Passos-Bueno, M. R., Cerqueira, A., et al. (2004). Asymptomatic carriers and gender differences in facioscapulohumeral muscular dystrophy (FSHD). Neuromuscul Disord, *14*, 33-38.

Tsang, L. W., Hu, N., and Underhill, D. A. (2010). Comparative Analyses of SUV420H1 Isoforms and SUV420H2 Reveal Differences in Their Cellular Localization and Effects on Myogenic Differentiation. PLoS One, *5*, e14447.

Tupler, R., Barbierato, L., Memmi, M., et al. (1998). Identical de novo mutation at the D4F104S1 locus in monozygotic male twins affected by facioscapulohumeral muscular dystrophy (FSHD) with different clinical expression. J Med Genet, *35*, 778-783.

Tupler, R., Perini, G., Pellegrino, M. A., et al. (1999). Profound misregulation of muscle-specific gene expression in facioscapulohumeral muscular dystrophy. Proc Natl Acad Sci U S A, *96*, 12650-12654.

van der Maarel, S. M., Tawil, R., and Tapscott, S. J. (2011). Facioscapulohumeral muscular dystrophy and DUX4: breaking the silence. Trends Mol Med, *17*, 252-258.

van Deutekom, J. C., Wijmenga, C., van Tienhoven, E. A., et al. (1993). FSHD associated DNA rearrangements are due to deletions of integral copies of a 3.2 kb tandemly repeated unit. Hum Mol Genet, *2*, 2037-2042.

van Koningsbruggen, S., Dirks, R. W., Mommaas, A. M., et al. (2004). FRG1P is localised in the nucleolus, Cajal bodies, and speckles. J Med Genet, *41*, e46.

van Koningsbruggen, S., Straasheijm, K. R., Sterrenburg, E., et al. (2007). FRG1P-mediated aggregation of proteins involved in pre-mRNA processing. Chromosoma, *116*, 53-64.

Wijmenga, C., Hewitt, J. E., Sandkuijl, L. A., et al. (1992). Chromosome 4q DNA rearrangements associated with facioscapulohumeral muscular dystrophy. Nat Genet, *2*, 26-30.

Winokur, S. T., Barrett, K., Martin, J. H., et al. (2003). Facioscapulohumeral muscular dystrophy (FSHD) myoblasts demonstrate increased susceptibility to oxidative stress. Neuromuscul Disord, *13*, 322-333.

Winokur, S. T., Chen, Y. W., Masny, P. S., et al. (2003). Expression profiling of FSHD muscle supports a defect in specific stages of myogenic differentiation. Hum Mol Genet, *12*, 2895-2907.

Wuebbles, R. D., Hanel, M. L., and Jones, P. L. (2009). FSHD region gene 1 (FRG1) is crucial for angiogenesis linking FRG1 to facioscapulohumeral muscular dystrophy-associated vasculopathy. Dis Model Mech, *2*, 267-274.

Xynos, A., Corbella, P., Belmonte, N., et al. (2011). Bone marrow-derived hematopoietic cells undergo myogenic differentiation following a Pax-7 independent pathway. Stem Cells, *28*, 965-973.

Xynos, A., Neguembor, M. V., Caccia, R., et al. (2013). Facioscapulohumeral muscular dystrophy region gene 1 over-expression causes primary defects of myogenic stem cells. Journal of cell science.

Yamashita, K., Sato, A., Asashima, M., et al. (2007). Mouse homolog of SALL1, a causative gene for Townes-Brocks syndrome, binds to A/T-rich sequences in pericentric heterochromatin via its C-terminal zinc finger domains. Genes to cells : devoted to molecular & cellular mechanisms, *12*, 171-182.

Zatz, M., Marie, S. K., Cerqueira, A., et al. (1998). The facioscapulohumeral muscular dystrophy (FSHD1) gene affects males more severely and more frequently than females. Am J Med Genet, *77*, 155-161.

FIGURE LEGENDS

Figure 1. FRG1 directly interacts with the histone methyltransferase Suv4-20h1. (**A**) Co-immunoprecipitation with anti-SUV4-20H1~~HA~~ shows that Myc-FRG1 interacts with ~~HA~~ SUV4-20H1. Immunoblots for Myc and ~~HA~~SUV4-20H1. (**B**) ~~Co-immunoprecipitation with anti-GFP shows that Myc-FRG1 interacts with GFP-Suv4-20h1. Immunoblots for Myc and GFP. (C)~~ GST pull-down assay demonstrates that FRG1 interacts directly with the C-terminus of Suv4-20h1. Recombinant 6xHis-FRG1 was specifically pulled down by GST-Suv4-20h1 full length and 385-874. Immunoblot for 6xHis. (~~D~~C) Schematic representation of Suv4-20h1 truncation constructs. (~~E~~D) His pull-down demonstrates that FRG1 interacts directly with the Suv4-20h1(509-630). Immunoblot for GST. Multiple bands in the first two lanes of the blots correspond to degradation products of Suv4-20h1 (~~F~~E) Co-immunoprecipitation with anti-HA shows that Myc-FRG1 co-immunoprecipitates with Suv4-20h1(509-630). Immunoblots for Myc and HA.

Figure 2. FRG1 over-expression alters the sub-nuclear distribution of SUV4-20H1.1.

(**A-D**) GFP fluorescence and immunofluorescence for Myc of C2C12 myoblasts transiently transfected with p*CMV-Myc-FRG1* or p*CMV-Myc* (in red) and p*EGFP-C1-SUV4-20H1.1*(A), p*EGFP-C1-SUV4-20H1.2* (B), p*EGFP-C1-SUV4-20H2* (C) or p*EGFP-N3* (D) (in green). Deconvoluted 0.1 µm sections at 60x magnification. Scale bars, 5 µm.

Figure 3. *FRG1* over-expression or *Suv4-20h1* knockdown inhibit muscle differentiation in C2C12 cells. Immunofluorescence for Myosin heavy chain (Mhc) (**A**) and fusion index analysis (**C**) shows that p*FH-FRG1* over-expressing cells display a significant decrease in the fusion index compared to control (p*FH*) (paired t test: p=0.0067, n=3) and untreated C2C12 cells (paired t test: p=0.0067, n=3). Mean ± SEM are shown. Immunofluorescence for Myosin heavy chain (Mhc) (**B**) and fusion index analysis (**D**) shows that *Suv4-20h1* knockdown (shRNA#1, 2 and 3) cells display a

significantly reduced myogenic differentiation compared to control shRNA expressing cells (one-way Anova test: p<0.0001, n=3, mean ± SEM). (**E**) Immunoblot performed on p*FH* and p*FH-FRG1* myoblasts (anti-FRG1, anti-HA and anti-Tubulin). (**F**) Immunoblot performed on control shRNA and Suv4-20h1 shRNA#1, 2 and 3 myoblasts (anti-Suv4-20h1 and anti-Tubulin. Scale bars, 200 µm.

Figure 4. *SUV4-20H1* over-expression partially rescues *FRG1* phenotype. Immunofluorescence for Myosin heavy chain (Mhc) (**A**) and fusion index analysis (**B**) show that 4-hydroxytamoxifen (4-OHT) induction of *SUV4-20H1_ERα*/p*FH-FRG1* cells leads to a specific and significant amelioration of the differentiation of *FRG1* over-expressing myotubes compared to control cells (two way Anova test, p= 0.0406; n=3, mean ± SEM) (**C**) Immunoblot performed in *SUV4-20H1_ERα*/p*FH-FRG1* and empty vector control/p*FH-FRG1* myoblasts (anti-ERα and anti-Tubulin). Scale bars, 200 µm.

Figure 5. Partial muscle-specific *Suv4-20h* knockout causes muscular dystrophy signs. **(A)** qPCR analysis for the *Suv4-20h1*^{flox} allele in *Suv4-20h1*$^{flox/-}$ mice *Cre*$^{+}$ or *Cre*$^{-}$ shows that the *Suv4-20h1*^{flox} allele is not completely excised in muscles from *Suv4-20h1*$^{-/-}$ mice (n≥4, mean ± SEM). **(B)** qRT-PCR analysis for *Suv4-20h1* in *Suv4-20h1*$^{flox/-}$ mice *Cre*$^{+}$ or *Cre*$^{-}$ displays a partial *Suv4-20h1* reduction in muscles from *Suv4-20h1*$^{-/-}$ mice (n≥4, mean ± SEM). **(C)** Immunofluorescence for H4K20me3 of tibialis anterior transverse cryosections from four-months old mice. **(DA–FC)** Gomori-trichrome staining of tibialis anterior transverse cryosections (AD). *mDKO* mouse muscles contain significantly more necrotic (EB; Mann-Whitney test: p=0.0079, n=5) and centrally-nucleated (C; Mann-Whitney test: p=0.0079, n=5) myofibers than *WT* controls. Error bars represent the standard error of the means of five animals. Scale bars, 100 µm.

Figure 6. *Eid3* is down-regulated upon muscle differentiation and behaves as myogenic inhibitor gene. (A) qRT-PCR shows that *WT* primary myoblasts express significantly higher *Eid3* levels than myotubes (unpaired t test: p<0.0001, n=3, mean ± SEM). **(B)** qRT-PCR for *Eid3* performed in C2C12 myoblasts and myotubes shows that C2C12 myoblasts express significantly higher levels of *Eid3* compared to myotubes (one sample t test: p=0.0052, n=3, mean ± SEM). (**C**) Immunofluorescence for Myosin Heavy Chain (Mhc) and (**D**) fusion index analysis shows that p*H-Eid3* over-expressing cells display a significantly decreased fusion index compared to control (p*FH*) (paired t test: p=0.0057, n=3, mean ± SEM). (**E**) Immunoblot performed on p*FH* and p*H-Eid3* myoblasts (anti-HA and anti-Tubulin).

Figure 7. The myogenic inhibitor gene *Eid3* is specifically over-expressed in FSHD and is an FRG1/Suv4-20h1 target. (A–F) qRT-PCR for *Eid3* in several biological samples. *Eid3* is significantly up-regulated in vastus from asymptomatic three-weeks old *FRG1* mice (A; paired t test: p=0.0039, n=5, mean ± SEM) compared to *WT* controls. *Eid3* levels are significantly increased in C2C12 muscle cells over-expressing *FRG1* (B; one sample t test: p=0.0025, n=4, mean ± SEM) compared to empty vector controls. *Eid3* expression is preferentially altered in severely affected muscles (*vastus lateralis*) compared to mildly affected muscles (*biceps brachii*) (C, paired t test: p=0.0086, n=3, mean ± SEM). *Eid3* is significantly more abundant in *mDKO* mice than *WT* controls (D; unpaired t test: p=0.0019, n=5, mean ± SEM). *Eid3* is significantly up-regulated in C2C12 muscle cells knockdown for *Suv4-20h1* (E; one sample t test: p=0.0039, n=4, mean ± SEM) compared to non-silencing control cells. *EID3* levels are significantly increased in FSHD muscle biopsies compared to healthy and other~~Becker~~ muscular dystrophy controls (F; one-way Anova test: p=0.0029~~485~~, n=7~~3~~–8~~4~~, mean ± SEM). (**G**) qRT-PCR for *FRG1* in several human muscle biopsies. *FRG1* is specifically over-expressed in FSHD patients compared to healthy and other muscular dystrophy controls (one-way Anova test: p=0.0013, n=7–8, mean ± SEM). (**H**) Pearson correlation analysis shows that *FRG1* and *EID3* expression levels are highly correlated (R^2=0.6611; p<0.0001,

n=22) (I~~G~~-J~~H~~) Chromatin immunoprecipitation, using total H4, H4K20me3 and IgG, as control antibodies. H4K20me3 is significantly reduced at the *Eid3* genomic region spanning -6 to -2 kb from TSS in *FRG1* over-expressing (G; two-way Anova test: p=0.0099, representative experiment, mean ± SEM) and *Suv4-20h1* knockdown (H; two-way Anova test: p=0.0043, representative experiment, mean ± SEM) C2C12 myotubes. H4K20me3 and IgG levels are relative to H4 and normalized by the H4K20me3 -6kb region enrichment levels of control samples (p*FH* and non silencing respectively).

Figure 8. *Eid3* knockdown rescues the myogenic capability of *FRG1* over-expressing cells. Immunofluorescence for Myosin Heavy Chain (Mhc) (**A**) and fusion index analysis (**B**; paired t test: p=0.0009, n=5, mean ± SEM) show that *Eid3* knockdown significantly ameliorates the differentiation capability of p*FH-FRG1* over-expressing cells (*Eid3* siRNA) compared to non-silencing control (control siRNA). (**C**) qRT-PCR analysis for *Eid3* in p*FH-FRG1*/*Eid3* siRNA displays a partial *Eid3* knockdown compared to p*FH-FRG1*/control siRNA (paired t test: p=0.0016, n=5, mean ± SEM). Scale bars, 200 μm. (**D**) Graphical representation of FRG1-overexpression proposed model.

Figure S1. FRG1 interacts with the murine and human histone methyltransferase Suv4-20h1. (**A**) Co-immunoprecipitation with anti-HA shows that Myc-FRG1 interacts with HA-SUV4-20H1. Immunoblots for Myc and HA. (**B**) Co-immunoprecipitation with anti-GFP shows that Myc-FRG1 interacts with GFP-Suv4-20h1. Immunoblots for Myc and GFP.

Figure S~~1~~2. The genetic interaction between FRG1 and Suv4-20h1 is evolutionarily conserved. (**A**) *Stubble* Position effect variegation (PEV) analysis performed in $T(2;3)Sb^{V}/TM3,Ser$ (Sb^{V}) shows that $Act5CGAL4;UAS\text{-}FRG1^{RNAi}/T(2;3)Sb^{V}$ ($FRG1^{RNAi}/Sb^{V}$) flies display a decreased number of *Stubble* bristles compared to control $T(2;3)Sb^{V}/TM3,Ser$ (Sb^{V}) flies (Fisher exact test: p<0.0001,

n=400 from 20 flies) as opposed to *Suv4-20*^{BG00814}/*T(2;3)Sb*^{V} (*Suv4-20*^{BG00814}/*Sb*^{V}) flies (Fisher exact test: p<0.0001, n=400 from 20 flies). Error bars represent the standard errors of the mean number of *Stubble* and *WT* bristles of 20 flies. (**B**) Representative image of *Stubble* (black arrow) and *WT* (green arrow) bristles. (**C**) Immunofluorescence for H4K20me3 of polytene chromosome spreads. (**D**) Densitometric analysis and quantification of H4K20me3 levels show that *FRG1*^{RNAi} flies display significantly increased levels of H4K20me3 compared to control *w1118* flies (unpaired t test: p<0.0001, n=5) as opposed to *Suv4-20*^{BG00814} (unpaired t test: p<0.0001, n=5), mean ± SEM are shown.

Figure S3~~2~~. H4K20me3 levels are unaltered in *FRG1* over-expressing cells and slightly reduced in *Suv4-20h1* knock-down C2C12 cells. Immunoblot for H4K20me3 and total H4 in protein extracts from *FRG1* over-expressing cells and *Suv4-20h1* knock-down cells and their relative controls at the myoblast and myotube stage.

~~***Suv4-20h1* Excision rate and expression analysis in *Suv4-20h mDKO* mouse (A) qPCR analysis for the *Suv4-20h1*^{flox} allele in *Suv4-20h1*$^{flox/-}$ mice *Cre*$^{+}$ or *Cre*$^{-}$ shows that the *Suv4-20h1*^{flox} allele is not completely excised in muscles from *Suv4-20h1*$^{-/-}$ mice (n≥4, mean ± SEM). (B) qRT-PCR analysis for *Suv4-20h1* in *Suv4-20h1*$^{flox/-}$ mice *Cre*$^{+}$ or *Cre*$^{-}$ displays a partial *Suv4-20h1* reduction in muscles from *Suv4-20h1*$^{-/-}$ mice (n≥4, mean ± SEM). (C) Immunofluorescence for H4K20me3 of tibialis anterior transverse cryosections from four-months-old mice. Scale bars, 100 µm~~

Figure S4~~3~~. qRT-PCR validation of differentially expressed genes in vastus muscles from pre-dystrophic, four-week-old *WT* and *FRG1* over-expressing mice. A selection of 56 differentially expressed genes obtained by Microarray analysis was validated using qRT-PCR. A heatmap of $\log_2$ fold change microarrays results (rigth side) and the corresponding $\log_2$ fold change qRT-PCR validation on independent animals (left side). Relative quantification for qRT-PCRs has been

calculated using qbasePLUS software and the relative quantification mean from 3 *WT* mice has been used for each ratio calculation.

Figure S5. *EID3* and *FRG1* are specifically over-expressed in FSHD compared to healthy subjects and other muscular dystrophy controls. (**A-D**) Scattered plots of qRT-PCR performed in human muscle biopsies samples from heathy subjects, FSHD patients and other muscular dystrophy patients. (A) qRT-PCR for *EID3* shows significant over-expression in FSHD compared to controls (one-way Anova: p=0.0029, n=7-8, mean ± SEM). (B) qRT-PCR for *FRG1* shows significant over-expression in FSHD compared to controls (one-way Anova: p=0.0013, n=7-8, mean ± SEM). (C) qRT-PCR for *SUV4-20H1* shows that *SUV4-20H1* levels are not significantly different in FSHD muscle compared to healthy and other muscular dystrophy controls (one-way Anova test: p=ns, n=7–8, mean ± SEM). (D) qRT-PCR for *β-glucuronidase* (*GUS*) shows that *SUV4-20H1* levels are not significantly different in FSHD muscle compared to healthy and other muscular dystrophy controls (one-way Anova test: p=ns, n=7–8, mean ± SEM).

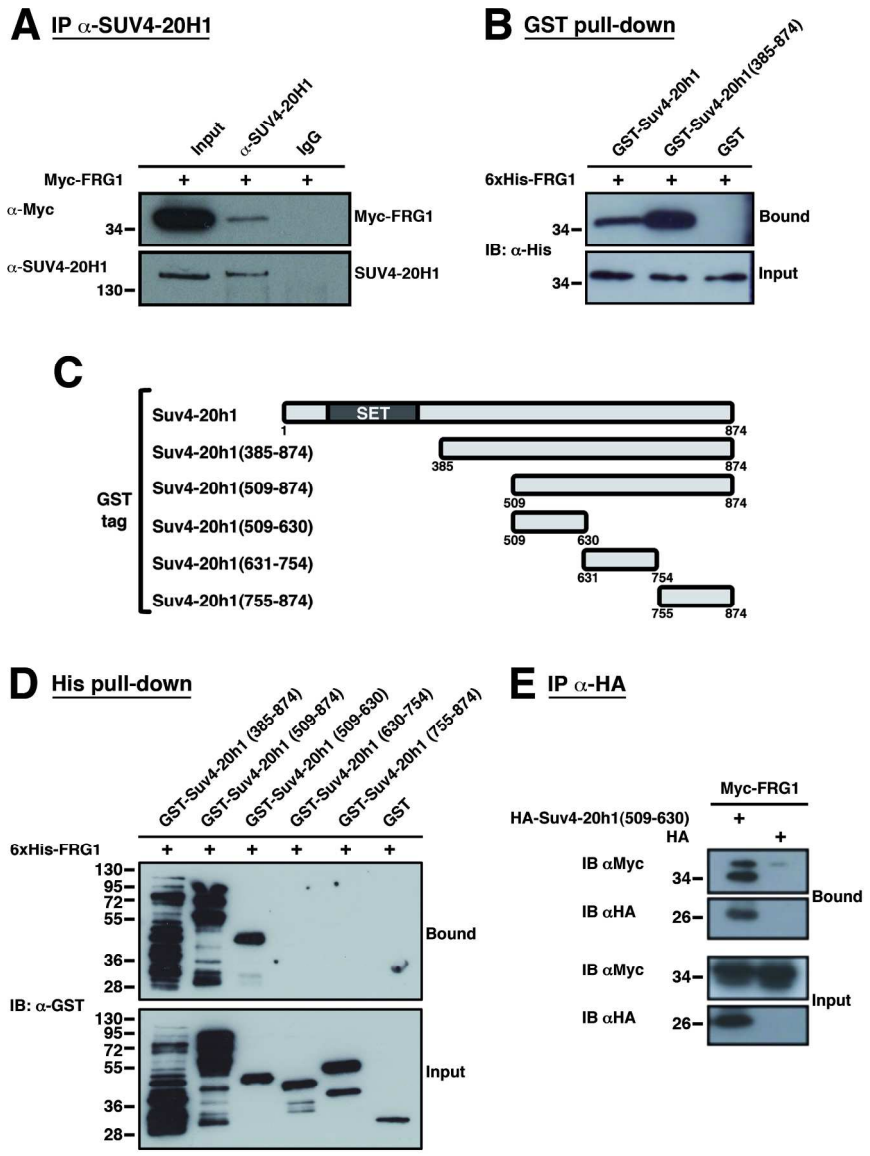

FRG1 directly interacts with the histone methyltransferase Suv4-20h1. (A) Co-immunoprecipitation with anti-SUV4-20H1 shows that Myc-FRG1 interacts with SUV4-20H1. Immunoblots for Myc and SUV4-20H1. (B) GST pull-down assay demonstrates that FRG1 interacts directly with the C-terminus of Suv4-20h1. Recombinant 6xHis-FRG1 was specifically pulled down by GST-Suv4-20h1 full length and 385-874. Immunoblot for 6xHis. (C) Schematic representation of Suv4-20h1 truncation constructs. (D) His pull-down demonstrates that FRG1 interacts directly with the Suv4-20h1(509-630). Immunoblot for GST. Multiple bands in the first two lanes of the blots correspond to degradation products of Suv4-20h1 (E) Co-immunoprecipitation with anti-HA shows that Myc-FRG1 co-immunoprecipitates with Suv4-20h1(509-630). Immunoblots for Myc and HA.
171x235mm (300 x 300 DPI)

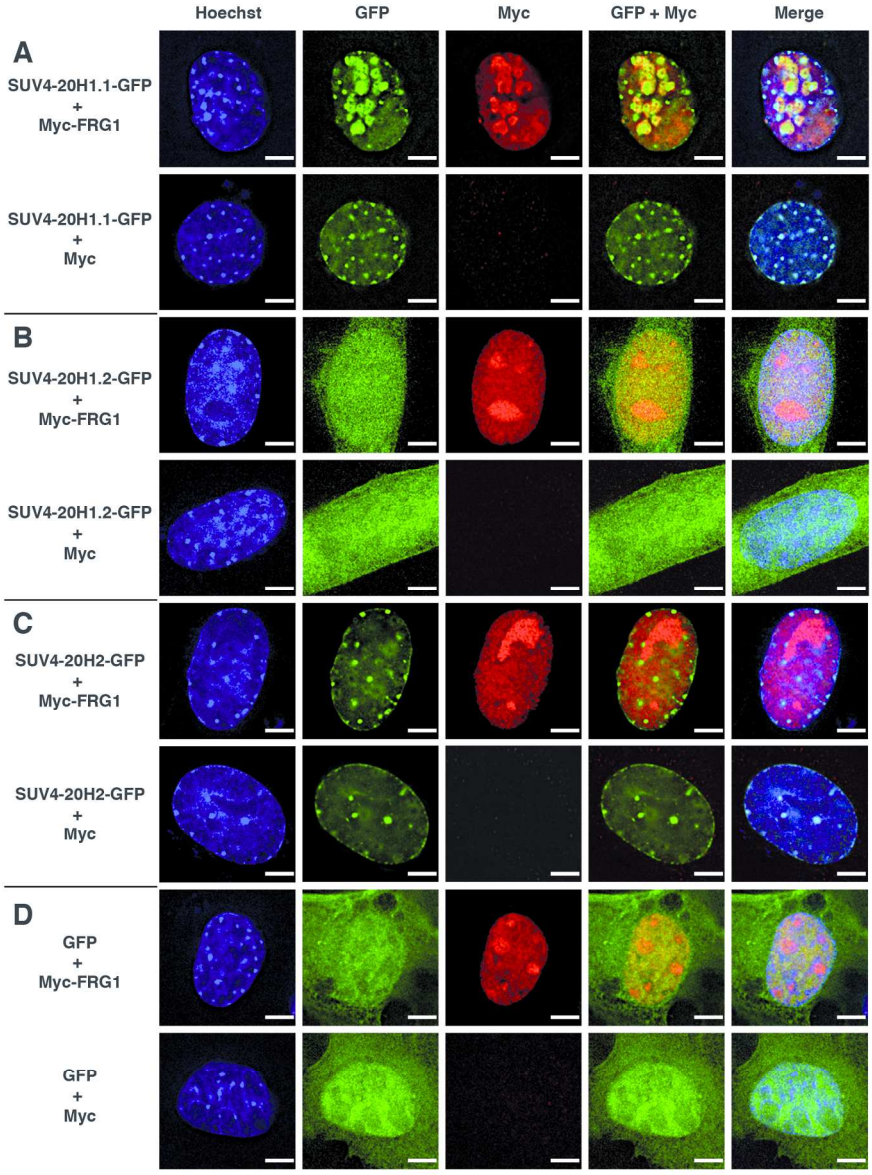

FRG1 over-expression alters the sub-nuclear distribution of SUV4-20H1.1.
(A-D) GFP fluorescence and immunofluorescence for Myc of C2C12 myoblasts transiently transfected with pCMV-Myc-FRG1 or pCMV-Myc (in red) and pEGFP-C1-SUV4-20H1.1(A), pEGFP-C1-SUV4-20H1.2 (B), pEGFP-C1-SUV4-20H2 (C) or pEGFP-N3 (D) (in green). Deconvoluted 0.1 µm sections at 60x magnification. Scale bars, 5 µm.
171x235mm (300 x 300 DPI)

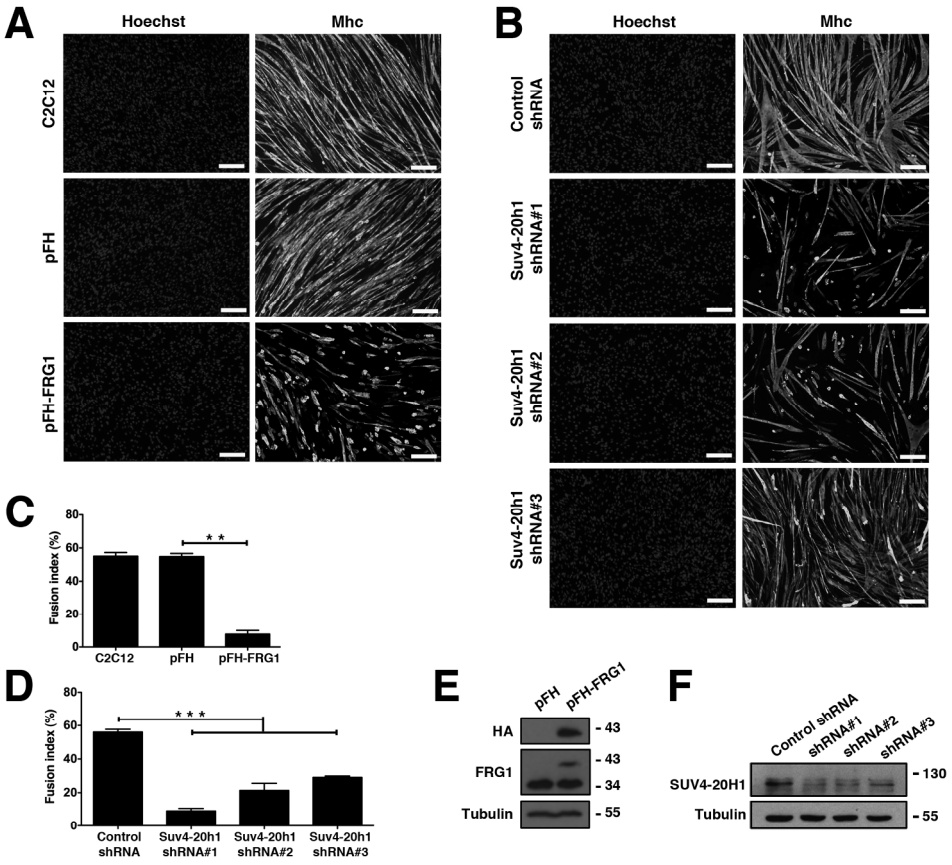

FRG1 over-expression or Suv4-20h1 knockdown inhibit muscle differentiation in C2C12 cells. Immunofluorescence for Myosin heavy chain (Mhc) (A) and fusion index analysis (C) shows that pFH-FRG1 over-expressing cells display a significant decrease in the fusion index compared to control (pFH) (paired t test: p=0.0067, n=3) and untreated C2C12 cells (paired t test: p=0.0067, n=3). Mean ± SEM are shown. Immunofluorescence for Myosin heavy chain (Mhc) (B) and fusion index analysis (D) shows that Suv4-20h1 knockdown (shRNA#1, 2 and 3) cells display a significantly reduced myogenic differentiation compared to control shRNA expressing cells (one-way Anova test: p<0.0001, n=3, mean ± SEM). (E) Immunoblot performed on pFH and pFH-FRG1 myoblasts (anti-FRG1, anti-HA and anti-Tubulin). (F) Immunoblot performed on control shRNA and Suv4-20h1 shRNA#1, 2 and 3 myoblasts (anti-Suv4-20h1 and anti-Tubulin. Scale bars, 200 μm.
197x185mm (300 x 300 DPI)

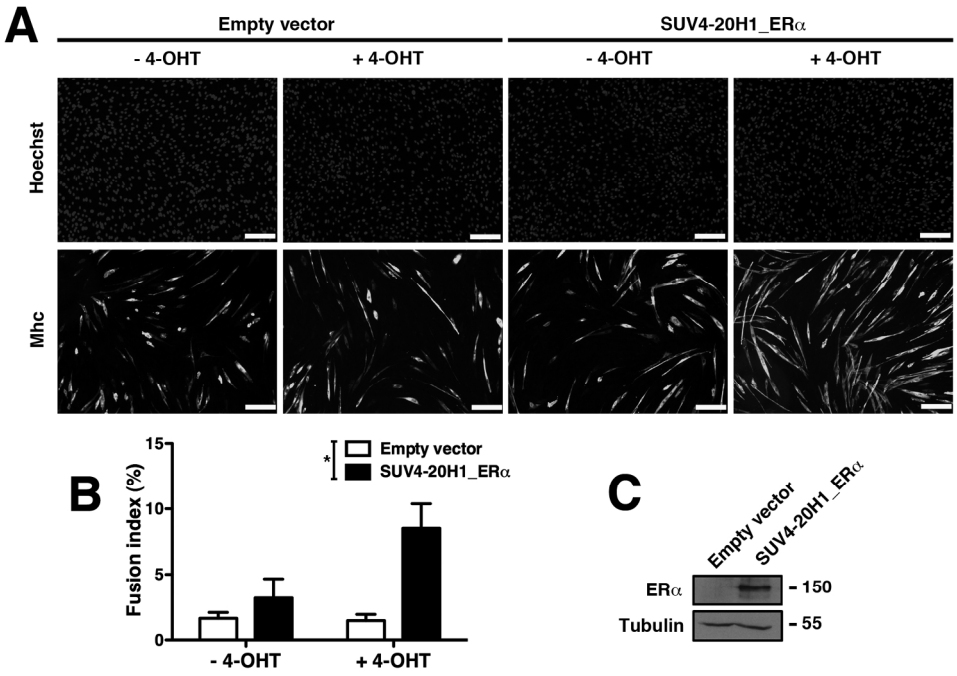

SUV4-20H1 over-expression partially rescues FRG1 phenotype. Immunofluorescence for Myosin heavy chain (Mhc) (A) and fusion index analysis (B) show that 4-hydroxytamoxifen (4-OHT) induction of SUV4-20H1_ERα/pFH-FRG1 cells leads to a specific and significant amelioration of the differentiation of FRG1 over-expressing myotubes compared to control cells (two way Anova test, p= 0.0406; n=3, mean ± SEM) (C) Immunoblot performed in SUV4-20H1_ERα/pFH-FRG1 and empty vector control/pFH-FRG1 myoblasts (anti-ERα and anti-Tubulin). Scale bars, 200 μm.
172x121mm (300 x 300 DPI)

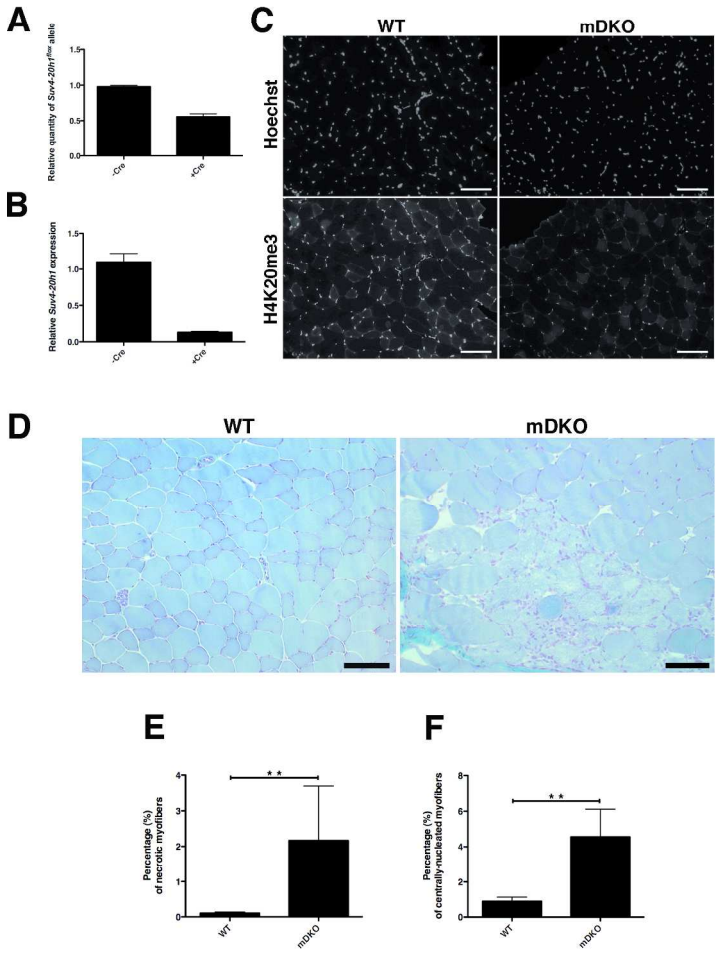

Partial muscle-specific Suv4-20h knockout causes muscular dystrophy signs. (A) qPCR analysis for the Suv4-20h1flox allele in Suv4-20h1flox/- mice Cre+ or Cre- shows that the Suv4-20h1flox allele is not completely excised in muscles from Suv4-20h1-/- mice (n≥4, mean ± SEM). (B) qRT-PCR analysis for Suv4-20h1 in Suv4-20h1flox/- mice Cre+ or Cre- displays a partial Suv4-20h1 reduction in muscles from Suv4-20h1-/- mice (n≥4, mean ± SEM). (C) Immunofluorescence for H4K20me3 of tibialis anterior transverse cryosections from four-months old mice. (D–F) Gomori-trichrome staining of tibialis anterior transverse cryosections (D). mDKO mouse muscles contain significantly more necrotic (E; Mann-Whitney test: p=0.0079, n=5) and centrally-nucleated (C; Mann-Whitney test: p=0.0079, n=5) myofibers than WT controls. Error bars represent the standard error of the means of five animals. Scale bars, 100 µm.
209x297mm (300 x 300 DPI)

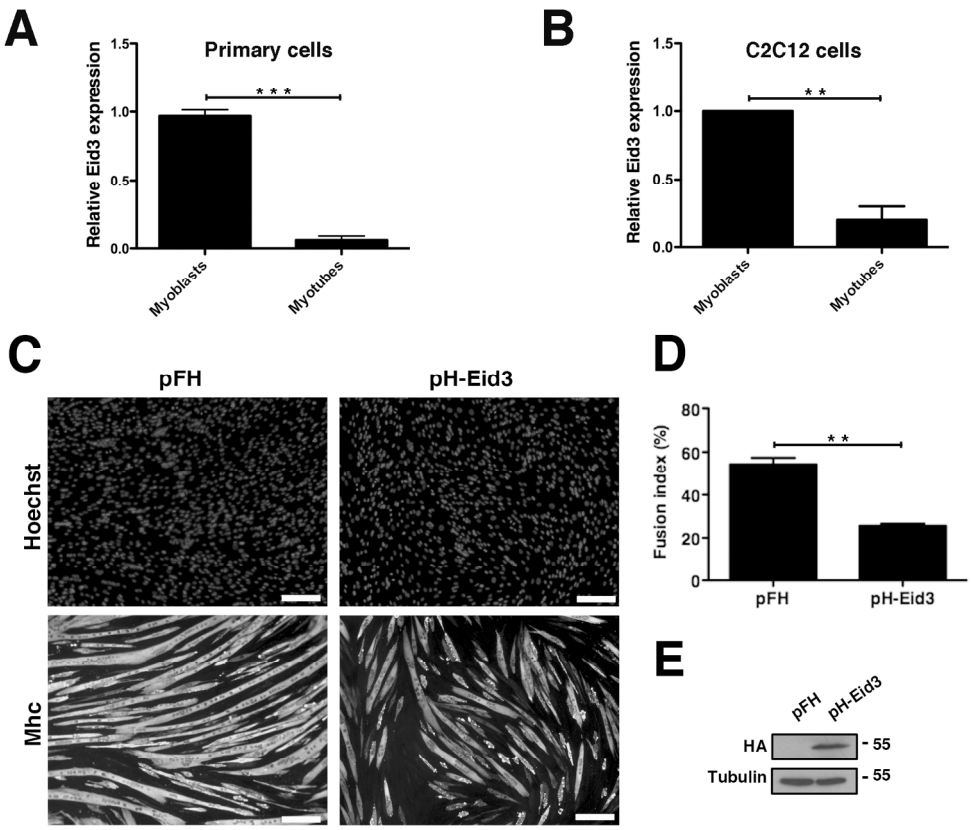

Eid3 is down-regulated upon muscle differentiation and behaves as myogenic inhibitor gene. (A) qRT-PCR shows that WT primary myoblasts express significantly higher Eid3 levels than myotubes (unpaired t test: $p<0.0001$, n=3, mean ± SEM). (B) qRT-PCR for Eid3 performed in C2C12 myoblasts and myotubes shows that C2C12 myoblasts express significantly higher levels of Eid3 compared to myotubes (one sample t test: $p=0.0052$, n=3, mean ± SEM). (C) Immunofluorescence for Myosin Heavy Chain (Mhc) and (D) fusion index analysis shows that pH-Eid3 over-expressing cells display a significantly decreased fusion index compared to control (pFH) (paired t test: $p=0.0057$, n=3, mean ± SEM). (E) Immunoblot performed on pFH and pH-Eid3 myoblasts (anti-HA and anti-Tubulin).
171x147mm (300 x 300 DPI)

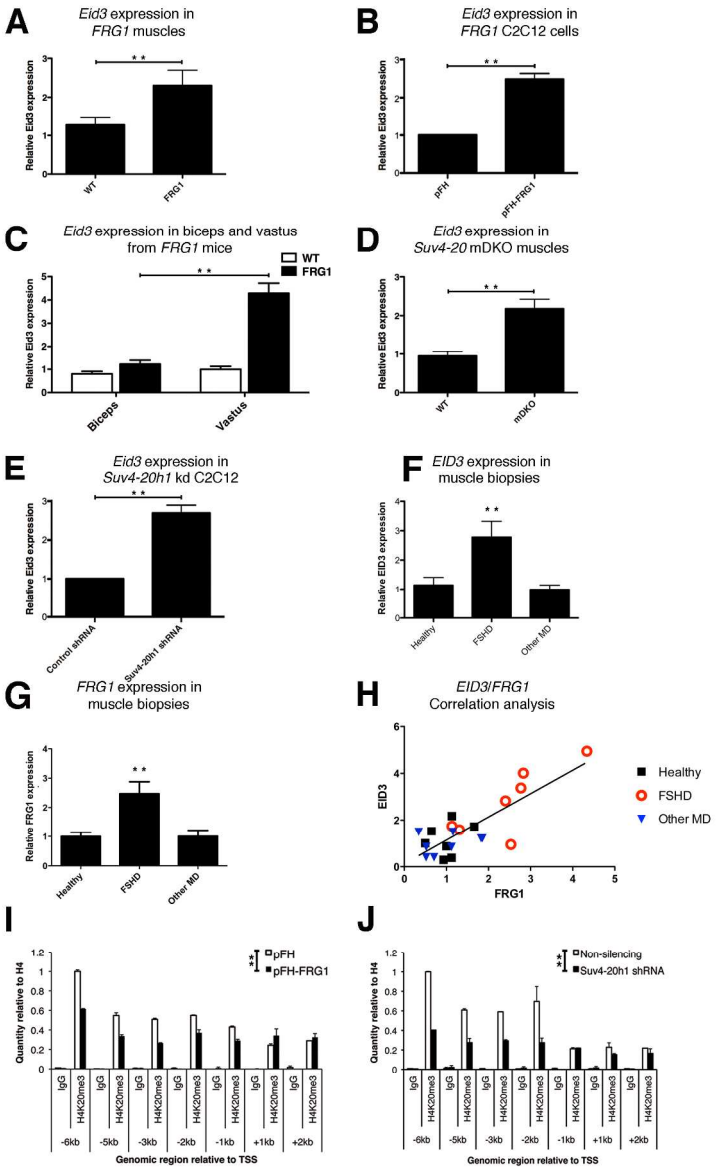

The myogenic inhibitor gene Eid3 is specifically over-expressed in FSHD and is an FRG1/Suv4-20h1 target. (A–F) qRT-PCR for Eid3 in several biological samples. Eid3 is significantly up-regulated in vastus from asymptomatic three-weeks old FRG1 mice (A; paired t test: p=0.0039, n=5, mean ± SEM) compared to WT controls. Eid3 levels are significantly increased in C2C12 muscle cells over-expressing FRG1 (B; one sample t test: p=0.0025, n=4, mean ± SEM) compared to empty vector controls. Eid3 expression is preferentially altered in severely affected muscles (vastus lateralis) compared to mildly affected muscles (biceps brachii) (C, paired t test: p=0.0086, n=3, mean ± SEM). Eid3 is significantly more abundant in mDKO mice than WT controls (D; unpaired t test: p=0.0019, n=5, mean ± SEM). Eid3 is significantly up-regulated in C2C12 muscle cells knockdown for Suv4-20h1 (E; one sample t test: p=0.0039, n=4, mean ± SEM) compared to non-silencing control cells. EID3 levels are significantly increased in FSHD muscle biopsies compared to healthy and other muscular dystrophy controls (F; one-way Anova test: p=0.0029, n=7–8, mean ± SEM). (G) qRT-PCR for FRG1 in several human muscle biopsies. FRG1 is specifically over-expressed in FSHD patients compared to healthy and other muscular dystrophy controls (one-way Anova test: p=0.0013, n=7–

8, mean ± SEM). (H) Pearson correlation analysis shows that FRG1 and EID3 expression levels are highly correlated (R2=0.6611; p<0.0001, n=22) (I-J) Chromatin immunoprecipitation, using total H4, H4K20me3 and IgG, as control antibodies. H4K20me3 is significantly reduced at the Eid3 genomic region spanning -6 to -2 kb from TSS in FRG1 over-expressing (G; two-way Anova test: p=0.0099, representative experiment, mean ± SEM) and Suv4-20h1 knockdown (H; two-way Anova test: p=0.0043, representative experiment, mean ± SEM) C2C12 myotubes. H4K20me3 and IgG levels are relative to H4 and normalized by the H4K20me3 -6kb region enrichment levels of control samples (pFH and non silencing respectively).
209x297mm (300 x 300 DPI)

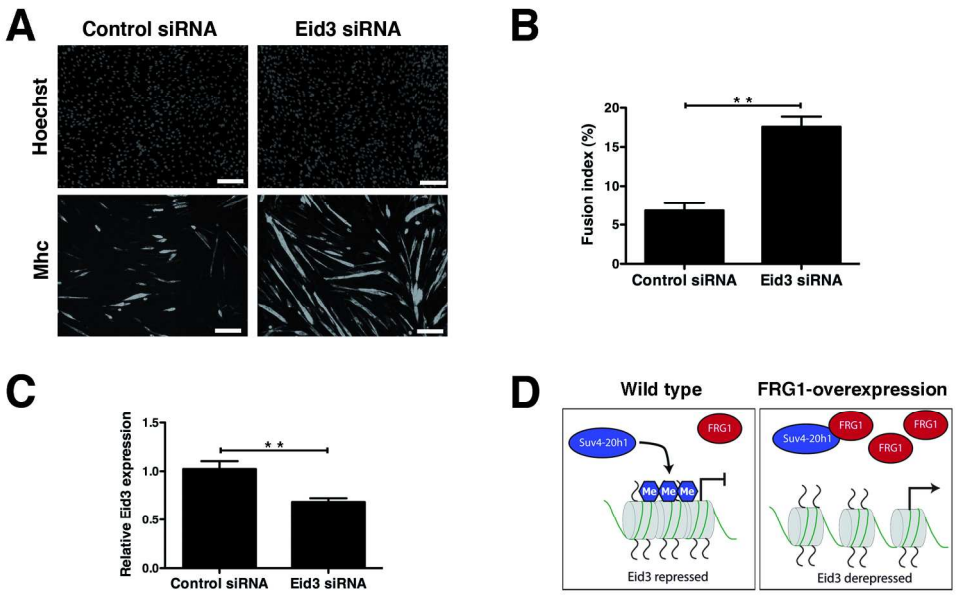

Eid3 knockdown rescues the myogenic capability of FRG1 over-expressing cells. Immunofluorescence for Myosin Heavy Chain (Mhc) (A) and fusion index analysis (B; paired t test: p=0.0009, n=5, mean ± SEM) show that Eid3 knockdown significantly ameliorates the differentiation capability of pFH-FRG1 over-expressing cells (Eid3 siRNA) compared to non-silencing control (control siRNA). (C) qRT-PCR analysis for Eid3 in pFH-FRG1/Eid3 siRNA displays a partial Eid3 knockdown compared to pFH-FRG1/control siRNA (paired t test: p=0.0016, n=5, mean ± SEM). Scale bars, 200 μm. (D) Graphical representation of FRG1-overexpression proposed model.
193x121mm (300 x 300 DPI)

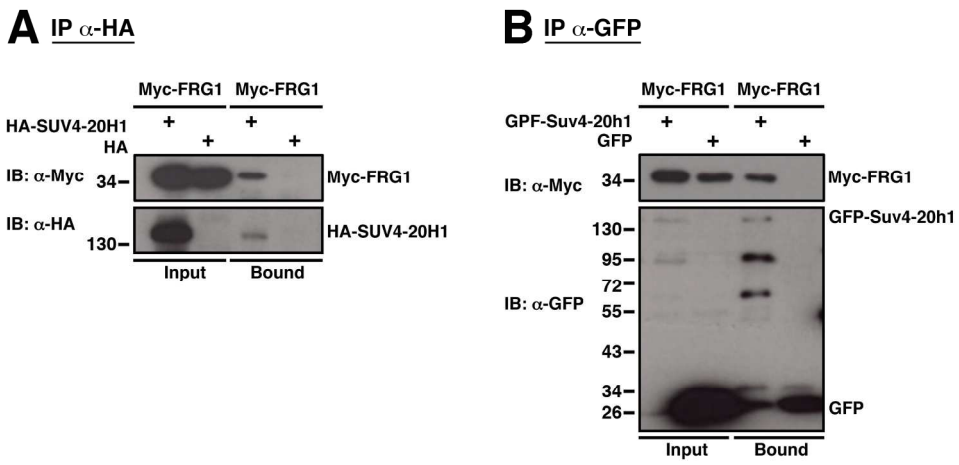

FRG1 interacts with the murine and human histone methyltransferase Suv4-20h1. (A) Co-immunoprecipitation with anti-HA shows that Myc-FRG1 interacts with HA-SUV4-20H1. Immunoblots for Myc and HA. (B) Co-immunoprecipitation with anti-GFP shows that Myc-FRG1 interacts with GFP-Suv4-20h1. Immunoblots for Myc and GFP.
183x98mm (300 x 300 DPI)

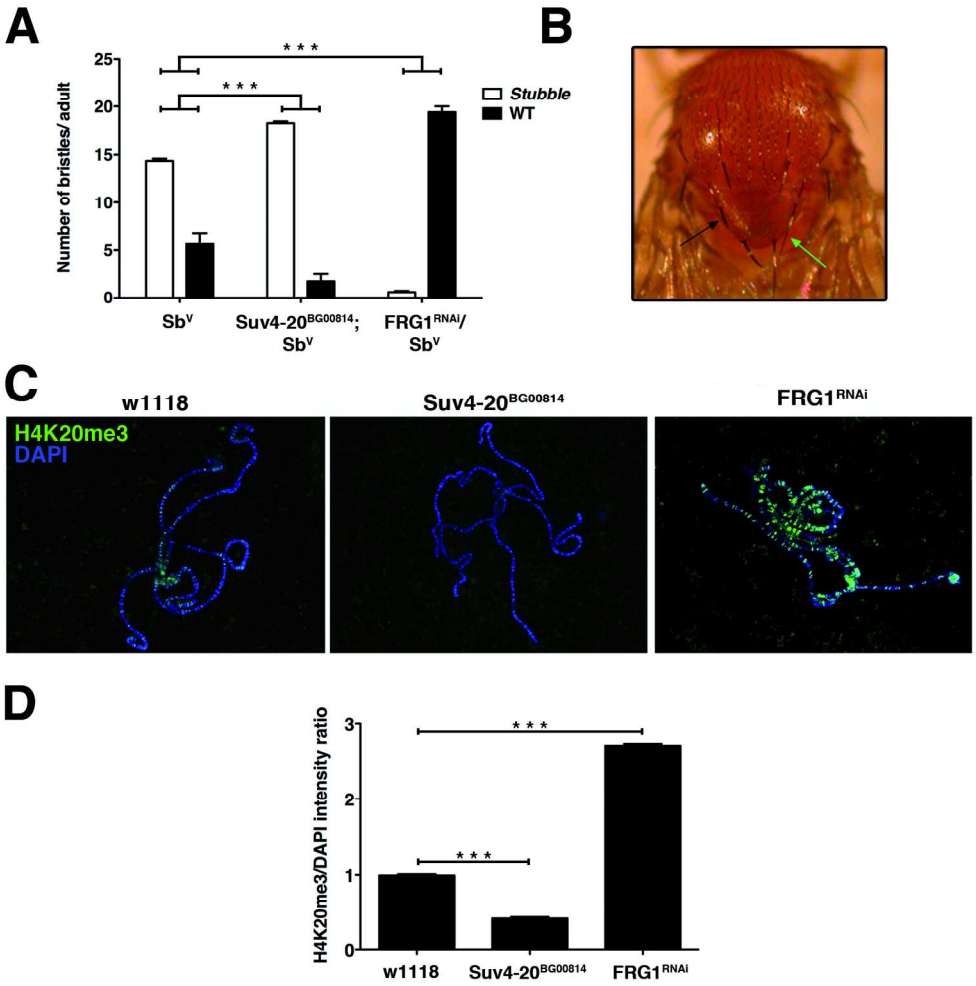

The genetic interaction between FRG1 and Suv4-20h1 is evolutionarily conserved. (A) Stubble Position effect variegation (PEV) analysis performed in T(2;3)SbV/TM3,Ser (SbV) shows that Act5CGAL4;UAS-FRG1RNAi/T(2;3)SbV (FRG1RNAi/SbV) flies display a decreased number of Stubble bristles compared to control T(2;3)SbV/TM3,Ser (SbV) flies (Fisher exact test: $p<0.0001$, n=400 from 20 flies) as opposed to Suv4-20BG00814/T(2;3)SbV (Suv4-20BG00814/SbV) flies (Fisher exact test: $p<0.0001$, n=400 from 20 flies). Error bars represent the standard errors of the mean number of Stubble and WT bristles of 20 flies. (B) Representative image of Stubble (black arrow) and WT (green arrow) bristles. (C) Immunofluorescence for H4K20me3 of polytene chromosome spreads. (D) Densitometric analysis and quantification of H4K20me3 levels show that FRG1RNAi flies display significantly increased levels of H4K20me3 compared to control w1118 flies (unpaired t test: $p<0.0001$, n=5) as opposed to Suv4-20BG00814 (unpaired t test: $p<0.0001$, n=5), mean ± SEM are shown.
171x171mm (300 x 300 DPI)

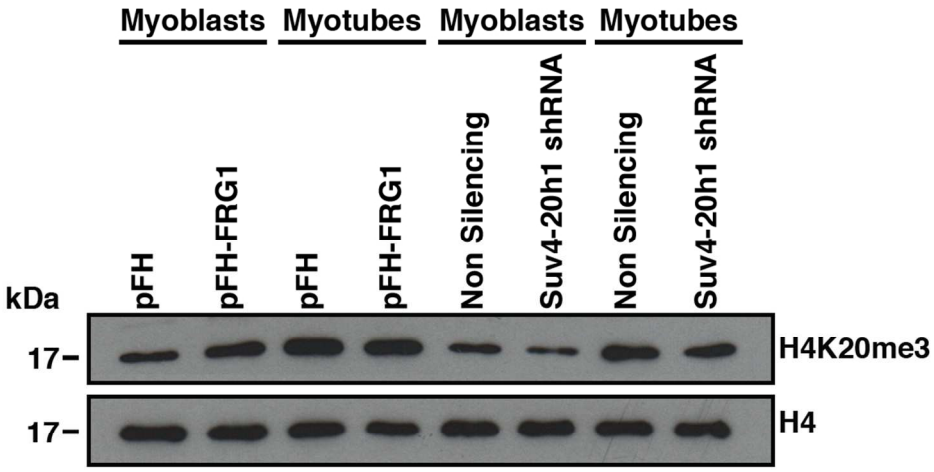

H4K20me3 levels are unaltered in FRG1 over-expressing cells and slightly reduced in Suv4-20h1 knock-down C2C12 cells. Immunoblot for H4K20me3 and total H4 in protein extracts from FRG1 over-expressing cells and Suv4-20h1 knock-down cells and their relative controls at the myoblast and myotube stage.
104x60mm (300 x 300 DPI)

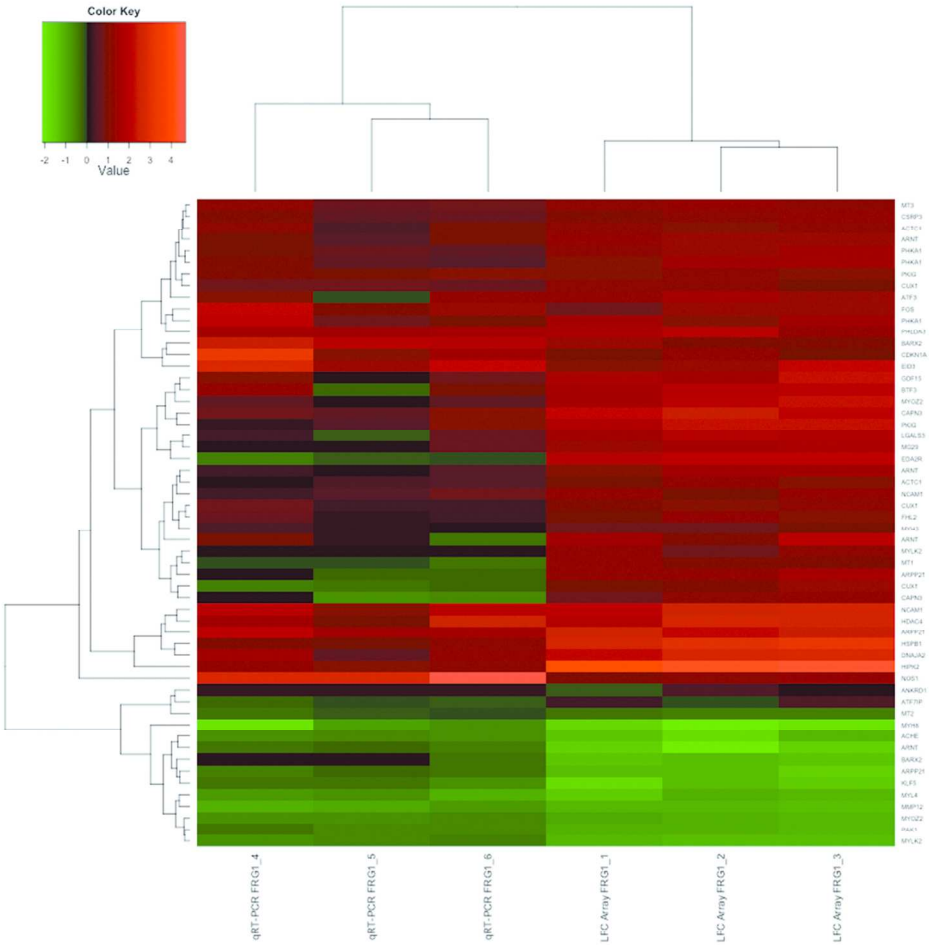

qRT-PCR validation of differentially expressed genes in vastus muscles from pre-dystrophic, four-week-old WT and FRG1 over-expressing mice. A selection of 56 differentially expressed genes obtained by Microarray analysis was validated using qRT-PCR. A heatmap of log2 fold change microarrays results (rigth side) and the corresponding log2 fold change qRT-PCR validation on independent animals (left side). Relative quantification for qRT-PCRs has been calculated using qbasePLUS software and the relative quantification mean from 3 WT mice has been used for each ratio calculation.
95x104mm (300 x 300 DPI)

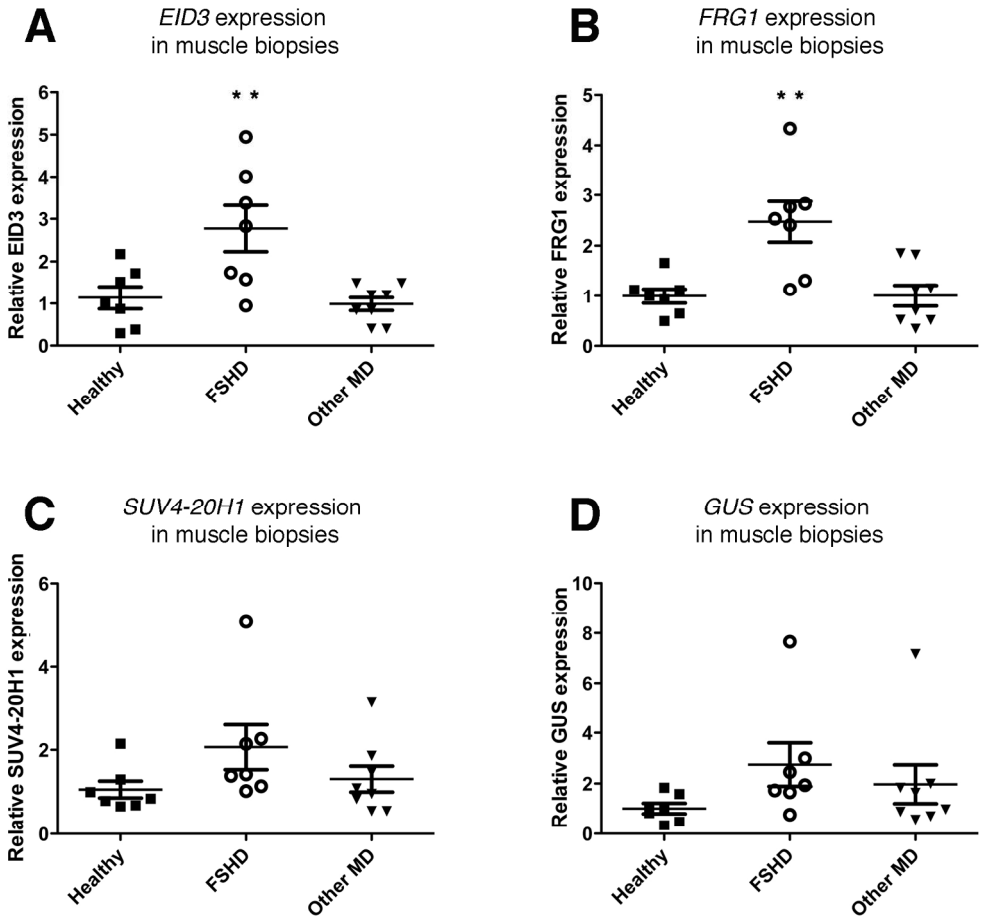

EID3 and FRG1 are specifically over-expressed in FSHD compared to healthy subjects and other muscular dystrophy controls. (A-D) Scattered plots of qRT-PCR performed in human muscle biopsies samples from heathy subjects, FSHD patients and other muscular dystrophy patients. (A) qRT-PCR for EID3 shows significant over-expression in FSHD compared to controls (one-way Anova: p=0.0029, n=7-8, mean ± SEM). (B) qRT-PCR for FRG1 shows significant over-expression in FSHD compared to controls (one-way Anova: p=0.0013, n=7-8, mean ± SEM). (C) qRT-PCR for SUV4-20H1 shows that SUV4-20H1 levels are not significantly different in FSHD muscle compared to healthy and other muscular dystrophy controls (one-way Anova test: p=ns, n=7–8, mean ± SEM). (D) qRT-PCR for β-glucuronidase (GUS) shows that SUV4-20H1 levels are not significantly different in FSHD muscle compared to healthy and other muscular dystrophy controls (one-way Anova test: p=ns, n=7–8, mean ± SEM).
184x176mm (300 x 300 DPI)

Supplementary Table I. Primers employed for cloning.

Construct	Primer	Sequence	Restriction site
p*CMV-HA-SUV4-20H1*	forward	5' aaGTCGAGgaagtggttgggagaatccaagaacatg 3'	*SalI*
	reverse	5' aaGCGGCCGCttaggcattaagccttaaagact 3'	*NotI*
p*CMV-HA-Suv420h1 (509-630)*	forward	5'aaGAATTCctaagaagaagaggaaggttggtcacaggca gaatcatgggagaggtg 3'	*EcoRI*
	reverse	5' aaCTCGAGtcagtctttcccagggaagctgtgctct 3'	*XhoI*
p*RSETA-FRG1*	forward	5' aaGGATCCgccgagtactcctatgtgaagtc 3'	*BamHI*
	reverse	5' aaGAATTCtcacttgcagtatctgtcggctttc 3'	*EcoRI*
p*GEX2T-Suv420h1 (509-874)*	forward	5' aaGGATCCcacaggcagaatcatgggagaggtg 3'	*BamHI*
	reverse	5' aaGAATTCtcatgcgttcagtcttagagactga 3'	*EcoRI*
p*GEX2T-Suv420h1 (509-630)*	forward	5' aaGGATCCcacaggcagaatcatgggagaggtg 3'	*BamHI*
	reverse	5' aaGAATTCtcagtctttcccagggaagctgtgctct 3'	*EcoRI*
p*GEX2T-Suv420h1 (631-754)*	forward	5' aaGGATCCgggctgccagatttgccagggtctc 3'	*BamHI*
	reverse	5' aaGAATTCtcacccgttactgagcttggcaacatag 3'	*EcoRI*
p*GEX2T-Suv420h1 (755-874)*	forward	5' aaGGATCCgtcagcgcagggccgggcagcagct 3'	*BamHI*
	reverse	5' aaGAATTCtcatgcgttcagtcttagagactga 3'	*EcoRI*
p*IRESneo3-HA-Eid3*	forward	5' ttaaGAATTCaatctaaagaaaaatgttcc 3'	*EcoRI*
	reverse	5' aattCTCGAGtctttaatatgagttttg 3'	*XhoI*

Supplementary Table II. Human biopsies related to experimental procedures.

Sample	Length of D4Z4	Sex	Age	Muscle
Healthy 1	-	-	40	Quadriceps femoris
Healthy 2	-	-	28	Quadriceps femoris
Healthy 3	-	-	28	Quadriceps femoris
Healthy 4	-	M	43	Biceps brachii
Healthy 5	-	F	38	Quadriceps femoris
Healthy 6	-	M	20	Triceps brachii
Healthy 7	-	F	54	Biceps brachii
FSHD 1	20 kb	F	27	Quadriceps femoris
FSHD 2	21 kb	F	29	Quadriceps femoris
FSHD 3	-	M	46	Quadriceps femoris
FSHD 4	32	M	56	Biceps brachii
FSHD 5	30	M	51	Biceps brachii
FSHD 6	27	M	29	Biceps brachii
FSHD 7	33	F	67	Biceps brachii
Other MD 1 Becker	-	M	23	Quadriceps femoris
Other MD 2 Becker	-	M	20	Quadriceps femoris
Other MD 3 Becker	-	M	37	Quadriceps femoris
Other MD 4 Becker	-	M	30	Quadriceps femoris
Other MD 5 Myotonic Dystrophy 1	-	M	45	Biceps brachii
Other MD 6	-	M	31	Biceps brachii

Calpainopathy				
Other MD 7 Dysferlinopathy	-	F	43	Biceps brachii
Other MD 8 Dysferlinopathy	-	F	61	Biceps brachii

Supplementary Table III. Primers for qPCRs.

Gene	Primer	Sequence	Function
GAPDH/ Gapdh	forward	5' TCAAGAAGGTGGTGAAGCAGG 3'	Reference
	reverse	5' ACCAGGAAATGAGCTTGACAAA 3'	Reference
FRG1/ Frg1	forward	5' AGTCCTCCAGAGCAGTTTAC 3'	Target
	reverse	5' AATAAAGCAGCTATTTGAGGC 3'	Target
FRG1 (for human biopsies)	forward	5' TCTACAGAGACGTAGGCTGTCA 3'	Target
	reverse	5' CTTGAGCACGAGCTTGGTAG 3'	Target
Eid3	forward	5' AGTTCCTGGTTTTGGCCTCT 3'	Target
	reverse	5' TCGCAGTCGCTAAATTCCTT 3'	Target
Suv4-20h1	forward	5' CAGAACAAAATGGAGCCAAGATAG 3'	Target
	reverse	5' CGACCAGTTGACACAAACTTAC 3'	Target
SUV4-20H1	forward	5' AAATCCAGAGTGGGACTGCC 3'	Target
	reverse	5' CTGAAGATTTTCGGTTAGAAGTTGC 3'	Target
EID3	forward	5' ATACCCGTGGCCGGCATGTT 3'	Target
	reverse	5' ACTTCGCCGCGTACTCGCTA 3'	Target
GUS (from Krom et al., 2012)	forward	5' CTCATTTGGAATTTTGCCGATT 3'	Target
	reverse	5' CCGAGTGAAGATCCCCTTTTTA 3'	Target
Suv420h1^{flox}	forward	5' TGGCGATTGAGCGGTACCG 3'	Target
	reverse	5' GCCTCACTCTCTGAGTGCTGGAATC 3'	Target